NASA/TM—2007–215187

Solution Growth and Characterization of Single Crystals on Earth and in Microgravity

M.D. Aggarwal, J.R. Currie, and B.G. Penn
Marshall Space Flight Center, Marshall Space Flight Center, Alabama

A.K. Batra and R.B. Lal
Alabama A&M University, Department of Physics, Normal, Alabama

December 2007

The NASA STI Program…in Profile

Since its founding, NASA has been dedicated to the advancement of aeronautics and space science. The NASA Scientific and Technical Information (STI) Program Office plays a key part in helping NASA maintain this important role.

The NASA STI program operates under the auspices of the Agency Chief Information Officer. It collects, organizes, provides for archiving, and disseminates NASA's STI. The NASA STI program provides access to the NASA Aeronautics and Space Database and its public interface, the NASA Technical Report Server, thus providing one of the largest collections of aeronautical and space science STI in the world. Results are published in both non-NASA channels and by NASA in the NASA STI Report Series, which includes the following report types:

- TECHNICAL PUBLICATION. Reports of completed research or a major significant phase of research that present the results of NASA programs and include extensive data or theoretical analysis. Includes compilations of significant scientific and technical data and information deemed to be of continuing reference value. NASA's counterpart of peer-reviewed formal professional papers but has less stringent limitations on manuscript length and extent of graphic presentations.

- TECHNICAL MEMORANDUM. Scientific and technical findings that are preliminary or of specialized interest, e.g., quick release reports, working papers, and bibliographies that contain minimal annotation. Does not contain extensive analysis.

- CONTRACTOR REPORT. Scientific and technical findings by NASA-sponsored contractors and grantees.

- CONFERENCE PUBLICATION. Collected papers from scientific and technical conferences, symposia, seminars, or other meetings sponsored or cosponsored by NASA.

- SPECIAL PUBLICATION. Scientific, technical, or historical information from NASA programs, projects, and missions, often concerned with subjects having substantial public interest.

- TECHNICAL TRANSLATION. English-language translations of foreign scientific and technical material pertinent to NASA's mission.

Specialized services also include creating custom thesauri, building customized databases, and organizing and publishing research results.

For more information about the NASA STI program, see the following:

- Access the NASA STI program home page at <http://www.sti.nasa.gov>

- E-mail your question via the Internet to <help@sti.nasa.gov>

- Fax your question to the NASA STI Help Desk at 301–621–0134

- Phone the NASA STI Help Desk at 301–621–0390

- Write to:
  NASA STI Help Desk
  NASA Center for AeroSpace Information
  7115 Standard Drive
  Hanover, MD 21076–1320

NASA/TM—2007–215187

Solution Growth and Characterization of Single Crystals on Earth and in Microgravity

M.D. Aggarwal, J.R. Currie, and B.G. Penn
Marshall Space Flight Center, Marshall Space Flight Center, Alabama

A.K. Batra and R.B. Lal
Alabama A&M University, Department of Physics, Normal, Alabama

National Aeronautics and
Space Administration

Marshall Space Flight Center • MSFC, Alabama 35812

December 2007

Acknowledgments

The authors are grateful for helpful discussions with a number of graduate students and other faculty in the department of physics at Alabama A&M University. Authors are thankful to Garland Sharp for his expert machining work and Jerry Johnson for glass blowing in the design of various crystal growth systems described in this Technical Memorandum. This work was partially supported under the NSF–HBCU RISE Program, HRD–0531183 and the U.S. Army Space and Missile Defense Command contract W9113M–04–C–0005. M.D. Aggarwal and R.B. Lal, two of the authors, would like to acknowledge support from the NASA Administrator's Fellowship Program (NAFP) through the United Negro College Fund Special Programs (UNCFSP) Corporation under contract NNG06GC58A.

TRADEMARKS

Available from:

NASA Center for AeroSpace Information
7115 Standard Drive
Hanover, MD 21076–1320
301–621–0390

This report is also available in electronic form at
<https://www2.sti.nasa.gov>

TABLE OF CONTENTS

LIST OF FIGURES

LIST OF FIGURES (Continued)

LIST OF TABLES

LIST OF ACRONYMS AND SYMBOLS

APCF	advanced protein crystallization facility
ATGSP	L-alanine triglycine sulfophosphate
BCF	Burton, Cabrera, and Frank
DCAM	diffusion-controlled crystallization apparatus for microgravity
DGS	diglycine sulfate
DLATGS	deuterated L-alanine triglycine sulphate
DTGS	deuterated triglycine sulfate
EDTA	ethylene diamine tetra acetic acid
FES	fluid experiments system
HDPCG	high-density protein crystal growth
HH–PCAM	hand-held protein crystallization apparatus for microgravity
HOE	holographic optical elements
IML	International Microgravity Laboratory
KDP	potassium dihydrogen phosphate
KH_2PO_4	potassium dihydrogen phosphate
LAFB	L-arginine tetrafluoroborate
LAP	L-arginine phosphate
LHFB	L-histidine tetrafluoroborate
MAP	methyl amino propanol
MNA	methyl nitroaniline

LIST OF ACRONYMS (Continued)

NIST	National Institute of Standards and Technology
PCAM	protein crystallization apparatus for microgravity
PCF	protein crystallization facility
STS	Space Transportation Systems
SL–3	Spacelab 3
TGS	triglycine sulfate
VDC	volts of direct current

NOMENCLATURE

a	dimension of growth unit perpendicular to the step
c	actual concentration of the solution
C_i	impurity concentrations
C_p	heat capacity
C^*	equilibrium concentration at a given temperature
D^*	detectivity
F	flat
g	gravitational acceleration
G_r	Grashof number
I^*	number of molecules in microcluster
k	thermal conductivity Boltzmman constant
K	kinks
K	kinetic coefficient
K'	kinetic coefficient
Ka	temperature-dependent adsorption constant
L	distance over which the heat must be conducted
L	ledges
M_o	surrounding mother liquor
n	number of bonds formed

NOMENCLATURE (Continued)

r	radius of the nucleus
r^*	radius of the critical nucleus
R	face growth rate
R_e	Reynolds number
R_F	growth rate of F face
S	stepped
S	adsorption site supersaturation
T	terrace
T	temperature in K
ν	frequency of vibration off molecules/atoms on the surface kinematic viscosity
V	values of average growth rate
V_m	molar volume of the solvent
$V_{(001)}$	axial velocity
$V_{(100)}$	axial velocity
W	activation energy
W	total quantity of work
W_S	work required to form a surface
Wv	work required to form the bulk of the particle
β	thermal expansion coefficient
γ	interfacial tension
δ	solubility parameter

NOMENCLATURE (Continued)

ΔC	concentration driving force
ΔG	Gibbs free energy change
ΔGv	free energy change per unit volume
ΔH	molar enthalpy
ΔT	supercooling temperature difference between the horizontal surfaces separated by L
ΔU	molar energy of dissolution
θ	fraction of adsorbed sites
μ	chemical potential of crystalline phase
μ_o	chemical potential of surrounding mother liquor
ρ	density
σ	relative supersaturation
φ	binding energy per pair

TECHNICAL MEMEORANDUM

SOLUTION GROWTH AND CHARACTERIZATION OF SINGLE CRYSTALS ON EARTH AND IN MICROGRAVITY

1. INTRODUCTION

The growth of crystals with tailored physical and chemical properties, characterization of crystals with advanced instrumentation, and their eventual conversion into devices play a vital role in science and technology. Crystal growth is an important field of materials science that involves controlled phase transformation. Growth of crystals from solution at low temperature is one of the important techniques in the field of science—pharmaceutical, agriculture, and materials science. Crystal growth acts as a bridge between science and technology for practical applications. In the past few decades, there has been a growing interest in the crystal growth process, particularly in view of the increasing demand for materials for technological applications. The strong influence of single crystals in present day technology is evident from the recent advancements in the fields of semiconductors, transducers, infrared detectors, ultrasonic amplifiers, ferrites, magnetic garnets, solid-state lasers, nonlinear optic, piezoelectric, acousto-optic, photosensitive materials, and crystalline thin films for microelectronics and computer applications. All these developments could only be achieved due to the availability of single crystals such as silicon, germanium, gallium arsenide, and also with the discovery of nonlinear optical properties in some inorganic, semiorganic and organic crystals. Researchers have always been in the search of new materials for the growth of single crystals for new applications and modifying present crystals for various applications. Any crystal growth process is complex; it depends on many parameters that can interact. A complete description of a process may well be impossible, since it would require the specifications of too many variables. That is why, sometimes crystal growth is called art and science, but like other crafts it can provide great satisfaction after a successful crystal growth of a desired material.

The solid-state materials can be classified into single crystals, polycrystalline, and amorphous materials depending upon the arrangement of constituent molecules, atoms, or ions. An ideal crystal is one in which the surroundings of any atom would be exactly the same as the surroundings of every similar atom in three dimensions. Real crystals are finite and contain defects. The consistency of the characteristics of devices fabricated from a crystal depends on the homogeneity and defect contents of the crystals. Hence, the process of producing single crystals that offer homogeneous media in the atomic level with directional properties attracts more attention than any other process. The methods of growing crystals are mainly dictated by the characteristics of the material and the desired size of the crystal. The method of growing crystals at low and high temperature can be broadly divided into the following six categories:

- Growth from aqueous solution (low-temperature growth).
- Growth by gel method (low-temperature growth).
- Growth from flux or top-seeded solution growth method (high-temperature growth).

- Hydrothermal growth (high-temperature growth).
- High-pressure growth (high-temperature growth).
- Growth by electrodeposition.

Growth of bulk crystals from aqueous solution is technically very important. Besides bulk crystal growth, this method is also used for the purification of materials and the separation of impurities. Growth of large single crystals from aqueous solution is of interest for essentially two reasons: 1) There is a growing need for solution-grown crystals in the area of high-power laser technology, like potassium dihydrogen phosphate (KDP) type crystals and 2) research in this area of crystal growth and the corresponding in-depth examination of several key parameters provides fundamental case studies generating theory and technology applicable to all solution crystal growth processes, including new aqueous growth systems and high-temperature solution growth.

In this article, the fundamental aspects of solution growth and the different methods of bulk crystal growth from solution are described along with solution crystal growth in the microgravity environment of space. Based on the extensive experience of the authors in growing inorganic and organic crystals on Earth and in space, the authors have tried to give a lucid explanation of the funda-mentals of solution crystal growth and crystal growth systems. Enough details are given on crystallizer fabrication, associated instruments, and techniques so that a new researcher may be able to design and set up their own solution crystal growth system after review of this material. Furthermore, growth and perfection of technologically important crystal from aqueous solution, based on a case study of triglycine sulfate (TGS), is presented. Effects of various parameters such as the seed holder design; seed morphology; solution characteristics such as pH, growth temperature, dopants, and impurities; and microgravity on the physical properties are presented in detail.

2. CRYSTALLIZATION—NUCLEATION AND GROWTH KINETICS

The study and investigation of crystal growth implies the determination of growth laws, growth mechanisms, and explanation of final results, i.e. the crystal habit. These aspects are interconnected. Since the growth rate of a face depends on its growth mechanisms and contributes to define the crystal habit, the detailed knowledge of these aspects is essential for the production of crystals of specific physical or morphological properties. The crystal growth is due to deposition of solute particles on the crystal faces, which can grow layer by layer at different rates. The growth rate of a face, i.e. advancement of its surface in the normal direction per unit time, depends upon internal and external factors. Internal factors are the surface structure of faces, which in turn are related to the bulk crystal structure and their degree of perfection. Defects usually occur in the crystals and can emerge at the surface, affecting the growth kinetics. External factors are supersaturation, solute concentration that is related to solubility, temperature of the solution, solution composition, mechanical conditions such as still or stirred solution, presence of impurities, magnetic field, and gravitational field. The crystal growth of a face is a succession of complex processes, which take place at the interface between the liquid and solid phase. It therefore implies transport of matter and energy across the interface, which is the site of major importance in crystal growth.

In the following section, the fundamentals of nucleation and crystal growth at low-temperature solution are described.

2.1 Expression for Supersaturation

The supersaturation of a system can be expressed in a number of ways. A basic unit of concentration as well as temperature must be specified. The concentration driving force (ΔC), the supersaturation ratio (S), and relative supersaturation (σ) are related to each other as follows:

$$\Delta C = C - C^* \quad , \tag{1}$$

where C is the actual concentration of the solution and C^* is the equilibrium concentration at a given temperature.

The supersaturation ratio is given as,

$$S = C/C^* \quad . \tag{2}$$

The relative supersaturation is as follows:

$$\sigma = (C - C^*)/C^* \text{ or } \sigma = S - 1 \quad . \tag{3}$$

The supersaturation can be estimated if the concentration of a solution can be measured at a given temperature and the corresponding equilibrium saturation concentration is known.

The required supersaturation can be achieved either by cooling/evaporation or the addition of a precipitant. A detailed investigation on the relationship between supersaturation and spontaneous crystallization was reported by Meirs and Isaac.[1] The results of their analysis are shown in figure 1. There are three zones that are termed as region I, II, and III. The lower continuous line is the normal solubility of the salt concerned. The temperature and concentration at which spontaneous crystallization occurs, are represented by the upper broken curve, generally referred as the supersolubility curve. This curve is not well defined, like the solubility curve, and its position in the diagram depends on the degree of agitation of the solution. The three zones are defined as follows:

- Stable (undersaturated) zone, where crystallization is not possible.
- Metastable zone, where spontaneous crystallization is improbable. However, if a seed crystal is placed in such a metastable solution, growth will occur.
- Unstable or labile (supersaturation) zone, where spontaneous crystallization is more probable.

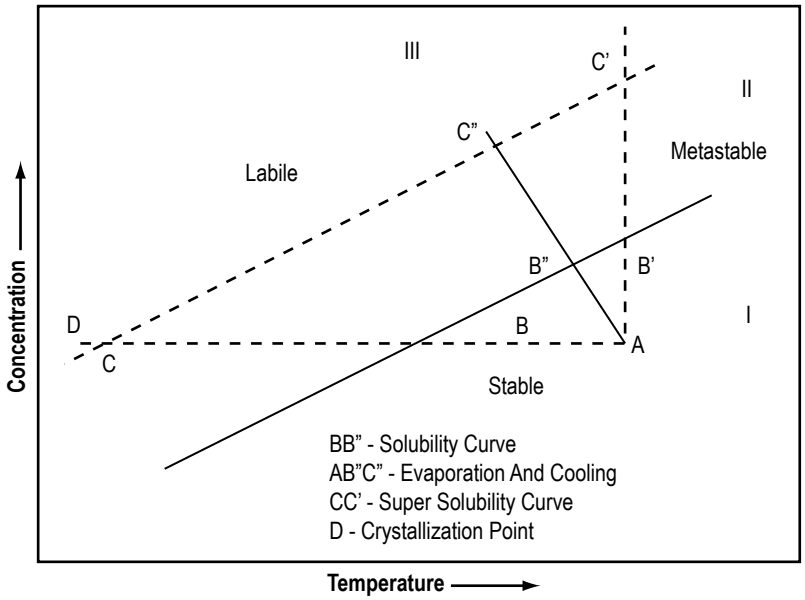

Figure 1. Meirs and Issac solubility curve.

The achievement of supersaturation is not sufficient to initiate the crystallization. Formation of embryos or nuclei with a number of minute solid particles present in the solution, often termed as centers of crystallization, is a prerequisite. Nucleation may occur spontaneously or it may be induced artificially. Broadly, nucleation can be classified into primary and secondary. All types of nucleation, homogeneous or heterogeneous, in systems that do not contain crystalline matter fall under primary. On the other hand, nucleation generated in the vicinity of crystals present in a supersaturated system is termed as secondary.

The formation of stable nuclei occurs only by the addition of molecule A_1, until a critical cluster is formed, as follows:

$$A_{n-1} + A_1 \rightarrow A_n \text{ (critical cluster)} \quad . \tag{4}$$

Subsequent additions to the critical cluster result in nucleation followed by growth. The growth units in a solution, ions or molecules, can interact with one another resulting in a short-lived cluster. Short chains or flat monolayers may be formed initially and eventually the lattice structure is built up. This process occurs very rapidly and continues in regions of very high supersaturation. Many nuclei fail to achieve maturity and simply dissolve due to their unstable nature. If the nuclei grow beyond a certain critical size, they become unstable under the average conditions of supersaturation in the bulk of the solution. The formation of a solid particle within a homogeneous solution results from the expenditure of a certain quantity of energy.

The total quantity of work (W) required for the formation of a stable nucleus is equal to the sum of the work required to form the surface (W_S), which is a positive quantity, and the work required to form the bulk of the particle (Wv) is a negative quantity as follows:

$$W = W_S + Wv \quad . \tag{5}$$

The change in Gibbs free energy (ΔG), between the crystalline phase and the surrounding mother liquor, results in a driving force that stimulates crystallization. This ΔG is the sum of the surface free energy and the volume free energy as

$$\Delta G \; = \; \Delta Gs \; + \; \Delta Gv \quad . \tag{6}$$

For a spherical nucleus,

$$\Delta G = 4\pi r^2\gamma + 4/3\, \pi r^3 \Delta Gv \quad , \tag{7}$$

where r is the radius of nucleus, γ is the interfacial tension, and ΔGv is the free-energy change per unit volume.

For rapid crystallization ($\Delta G < 0$) the first term in equation (7) expresses the formation of the new surface, and the second term expresses the difference in chemical potential between the crystalline phase (μ) and the surrounding mother liquor (μo). At the critical condition, free-energy formation obeys the condition $d\Delta G/dr = 0$. Hence, the radius of the critical nucleus is expressed as

$$r^* = 2\gamma/\Delta Gv \quad . \tag{8}$$

The critical free-energy barrier is

$$\Delta G^* = (16\, \pi\, \gamma^3\, v^2)/3(\Delta\mu)^2 \quad . \tag{9}$$

The number of molecules in the critical nucleus is given as follows:

$$I^* = 4/3\pi\gamma(r^*)^3 \quad . \tag{10}$$

The crucial parameter between a growing crystal and the surrounding mother liquor is the interfacial tension (γ). This complex parameter can be determined by conducting nucleation experiments.

Crystal growth from vapor, melt, or solution only occurs when the medium is supersaturated. The process involves at least two stages: 1) Formation of stable three-dimensional nuclei and (2) development of the stable three-dimensional nuclei into crystals with well-developed faces.[2]

The formation of three-dimensional nuclei is usually discussed in terms of reduction in the Gibbs free energy of the system. At a given supersaturation and temperature, there is a critical value of the free energy at which three-dimensional nuclei of a critical radius are formed. Only those nuclei that are greater than the critically sized nucleus are capable of growing into crystals of visible size by the attachment of growth species (i.e. molecules, atoms, or ions) at energetically favorable growth sites like kinks (K) in the ledges (L) of a surface. The surfaces of growing crystals may be flat (*F*), stepped (S), or kinked (K). Crystals of visible size are usually bound by the slowly growing *F* faces by the attachment of growth units at energetically favorable sites. Figure 2 shows different positions for the attachment of growth units at a flat crystal-medium interface of a simple cubic lattice. A growth unit attached at the surface terrace (T), a smooth L, and a K site has one, two, and three out of six nearest neighbors, respectively. Therefore, a growth unit arriving on the T, at the TL, and at the K simply loses one, two, and three degrees of freedom. If ϕ is the binding energy per pair, the corresponding binding energy of a growth unit attached at these sites is ϕ, 2ϕ and 3ϕ, respectively. Since the probability of capturing a growth unit at a given site depends on the term $exp(n\ \phi/kT)$, where n is the number of bonds formed, k is the Boltzmann constant, and T is the temperature in Kelvin the growth unit has a much higher probability of becoming a part of the crystal at the K site, rather than at the L or at the T.

Consequently, in contrast to Ls, the contribution of Ks is overwhelmingly high in the rate of displacement of a step along the surface (v), and in the rate of displacement of the surface normal to it (R). Similarly, the contribution to the face growth rate (R) by the direct attachment of growth units at the T is negligible.

From this discussion it may be concluded that the kinetics of crystal growth may, in general, be considered to occur in the following stages:

- Growth units transported to the growing surface by bulk diffusion and captured onto the T.
- Migration of growth units adsorbed onto the T to the S by surface diffusion and captured at the S.
- Migration of growth units adsorbed onto the S to the K site and integrated into the K.
- Transport of the released heat of the reaction and solvent molecules from the solvated atoms/molecules.

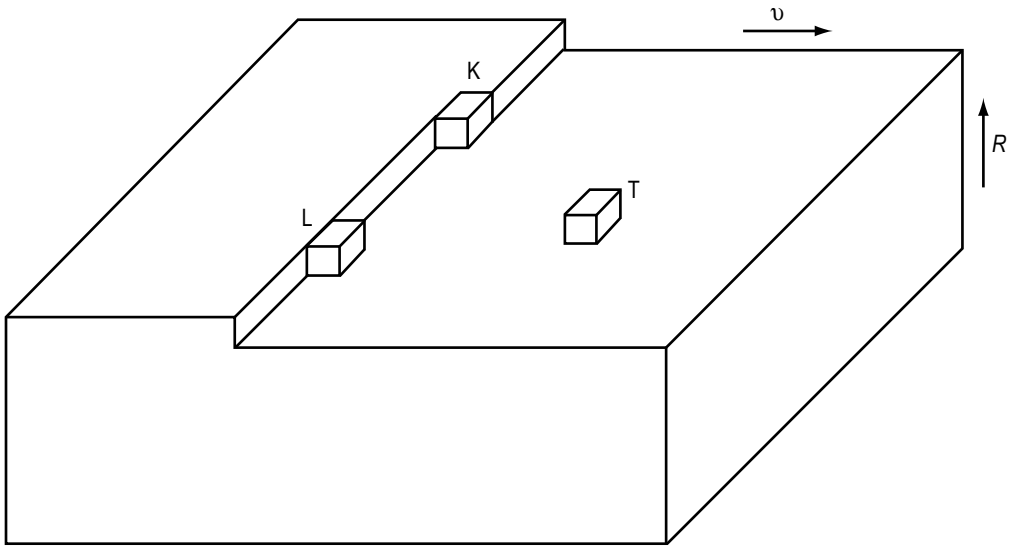

Figure 2. Different positions for the attachment of growth units at a flat crystal medium interface of a simple cubic lattice.

One or more of the above stages may control the growth rate, but the slowest one is always rate limiting. However, it should be noted that growth kinetics, characterized by rates v and R, depends on crystal structure, structure of crystal-medium interface (i.e. rough or smooth), presence of dislocations emerging on the growing face, supersaturation of the growth medium, growth temperature, stirring, and impurities present in the growth medium. It is also these factors that ultimately determine the surface morphology of crystals.

To explain the crystal growth processes, various theories and models along with the role of impurities, have been proposed in the past. For details, one can refer to various excellent references.[2–36] The important growth models are as follows:

- Two-dimensional nucleation models.
- Spiral growth models.
- Bulk diffusion models.
- Growth by a group of cooperating screw dislocations.

2.2 Effects of Convection in Solution Growth

Convection is comprised of two mechanisms: 1) Energy transfer due to random molecular motion (diffusion) and 2) energy transferred by the bulk or macroscopic motion of the fluid. This fluid motion is associated with the fact that, at any instance, large numbers of molecules are moving collectively or as aggregates. Such motion in the presence of a temperature gradient contributes to heat trans-

fer. Because the molecules in the aggregate retain their random motion, the total heat transfer is then due to a superposition of energy transport by the random motion of the molecules and by the bulk motion of the fluid. It is customary to use the term convection when referring to this cumulative transport and the term advection referring to transport due to bulk fluid motion.

2.2.1 Natural Convection

Convection heat flow can be classified as natural or free convection and forced convection, according to the nature of the fluid flow. Natural convection is due to the density difference of a solution near a crystal and far from it. Density difference is due primarily to the concentration change of a solution during growth or the dissolution of a crystal, and secondly to the absorption or evolution of the heat in the fluid. In natural convection, fluid motion is due to buoyancy forces within the fluid. Buoyancy is due to the combined presence of a fluid density gradient and a body force that is proportional to density. In practice, the body force is usually the gravitational force. Free-convection flows may occur in the form of a plume. The well-known convective flow pattern for solution growth is associated with fluid rising from the bottom of the crystal. Solution rises during the growth of a crystal because the solution near a crystal is less dense, resulting from the reduction in the concentration, and the temperature is higher because of the evolution of crystallization heat. With the depletion of the heavier solute, the solution around the crystal becomes lighter, and thus rises. When the crystal is dissolved, the direction of the motion is opposite (downward). Under these conditions, the diffusion of molecules is supplemented by the more energetic convective transport of matter.

Diffusion is the distribution of a substance by a random motion of individual particles. It is due to the presence of a gradient of the chemical potential in the system. A gradient is defined as an incremental of a function in an infinitely short distance along the direction of the most rapid variation of the function. Diffusion always reduces this gradient. Molecular diffusion is observed in viscous media and at low supersaturations, as well as in the growth of crystals, in thin films of liquids, or in capillaries. In molecular diffusion, the transport of matter to a crystal is slower than under other diffusion conditions. The thickness of the boundary layer increases with time and the concentration gradient gradually decreases. Therefore, the rate of growth decreases with time. The time interval during the formation of a boundary diffusion layer represents the nonsteady state condition. During this initial period, the rate of growth varies considerably. The thickness of the boundary layer depends on the difference between the densities of different parts of the solution (i.e., growth rate of a crystal), the viscosity of the solution, and the dimensions of the crystal. The presence of the boundary near the crystal, and the orientation of the crystal itself, affects the nature of the convection currents and the thickness of the boundary layer at different crystal faces.

2.2.2 Forced Convection

Forced convection is produced by the action of external forces, such as the forced motion of a crystal in solution. There is no basic difference between forced and natural convection. With respect to a crystal, when the motion velocity of a solution is increased, the thickness of the boundary layer increases and the supply of matter to a face of the crystal increases. Therefore, increasing the rate of motion of a solution increases the growth rate of the crystal faces; however, this processing cannot continue indefinitely. A temperature gradient constitutes the driving potential for heat transfer. Similarly, concentration gradient

of a species in a mixture or solution provides the driving potential of mass transfer. Both conduction heat transfer and mass diffusion are transport processes that originate from molecular activities. Crystal growers are actually concerned with two aspects of the nutrient-to-crystal transport: 1) The mass flux across an interface, referred to as interfacial flux, which determines the crystal growth rate; and 2) the concentration profile of growth species in the nutrient adjacent to the crystal, which is an essential parameter in morphological stability discussions.

Let us now introduce the dimensionless numbers that govern forced convection and free convection. The Grashof number (G_r) is as follows:

$$G_r = \frac{g\beta\Delta T \quad L^3}{v^2} \quad , \tag{11}$$

where g is gravitational acceleration (m/s^2), β is thermal expansion coefficient (β=1/ϱ($\delta\varrho/\delta T$), ϱ is density, ΔT is temperature difference between the horizontal surfaces separated by L, and v is kinematic viscosity (m^2/s). The Grashof number (G_r) plays the same role in free convection that the Reynolds number (R_e) plays in forced convection. The Reynold number (R_e) is shown as follows:

$$R_e = VL/v = \varrho VL/\mu \quad , \tag{12}$$

where V is velocity (m/s), L is characteristic length (m), v is kinematic viscosity (m^2/s), ϱ is density, and μ is viscosity (kg/s.m). The Reynolds number (R_e) provides a ratio of the inertial to viscous forces acting on a fluid element ratio. In contrast, the Grashof number (G_r) indicates the ratio of buoyancy force to viscous force acting on the fluid.

2.3 Effect of Impurities

We will now define impurities that are inherently present and additives, or dopants, which are deliberately added. The former are naturally present in the growth environment and are unwanted; the latter are deliberately added to control nucleation, improve crystal quality, increase size, and change the crystal habit and other physical properties. This topic has received great attention since it is of relevant theoretical and practical interest in the growth of crystals of industrial importance. The ability of impurities to change the growth behavior has been studied by many authors.[23–36] It is well known that the influence of impurities and the growth rate are based on the adsorption of foreign species (ions, atoms, or molecules) at Ks, Ls, and s of a growing crystal. The change of the crystal form is based on a difference in adsorption energies on different faces. Impurity molecules will be adsorbed preferentially on surfaces where the free adsorption energy has the maximum. It has been possible to predict the preferred surface using computational approaches.[37] Recently, the mechanisms and models of adsorption of impurities during the growth of bulk crystals have been surveyed by Sangwal, including kinetic effects of impurities on the growth of single crystals from solution.[36]

Solvent itself is an impurity. High temperatures and high supersaturations increase growth rate; but in the presence of a solvent, the effect of temperature is stronger since it promotes water desorption and growth kinetics much more than supersaturation, as found for sucrose.[38–39] Anomalies found by Chernov, et al. at 10 and 40 °C in growth rates disappeared when ethanol, which is known to disrupt the bulk structure of water, was added to the solution.[40] Indeed, water adsorbed on crystal surfaces has

properties differing from those of free water. This is attributed to the different structures of the adsorbed layer that undergo phaselike transformations at these temperatures.

Impurity adsorption can be indirectly studied though the adsorption isotherm, i.e. the fraction θ of adsorbed sites that are occupied as the impurity concentrations Ci increase. The simplest model of localized adsorption, i.e. situated at lattice sites, is the following Langmuir isotherm:

$$K_a\, Ci = \theta / (1 + \theta) \ , \tag{13}$$

where K_a is the temperature-dependent adsorption constant that is different for each crystal face. Other models have been proposed that take into account the interactions between adsorbed impurities or the occupation probability.

Impurities can act in different ways. When they interact with solute or solvent, they can have strong influences on solubility, and consequently on supersaturation and kinetic processes. When impurities are adsorbed on crystals they can have thermodynamic and kinetic effects. The dominant effect is the exchange rates in which the adsorbed molecule or ions and growth units are involved. If the former are exchanged more rapidly than the latter, adsorption mainly affects surface and edge-free energy. For a face, a decrease of γi (interfacial energy of face i) results, according to the following Gibb's equation:

$$\Delta\gamma i = kT\, In(1-\theta)/S \ , \tag{14}$$

where S is the area of the adsorption site. Similarly, the edge-free energy is decreased. These effects should cause an increase in the nucleation and growth rate. If the exchange rate of the adsorbed molecules is slower, impurities can strongly decrease the kinetic coefficients ($R_F=K\sigma^2$ at low super-saturation and $R_F=K'\sigma$ at high supersaturation), where K and K', kinetic coefficients, values depend on temperature and growth mechanisms; R_F is growth rate of F face; and σ is the relative supersaturation. So that as a final result the kinetic effects dominate the thermodynamic ones and a decrease in growth rate and impingement flux occur. The interpretation of impurity effects can be done on a structural and kinetic basis as follows:

- Low impurity concentrations can form an adsorbed monolayer on the surface, even in undersaturated solutions, due to a structural relationship between the two-dimensional structure of the crystal face and the adsorbed layer, as in the case of NaCl grown in the presence of $CdCl_2$ forms a monolayer of $Na_2CdCl_2 3H_2O$. The main influence is on the crystal habit.

- Kinetic interpretation considers the possibility of adsorption on the different surface sites. If impurities are adsorbed in the Ks, the advancement rate of the edge is hindered, even at very low impurity concentrations, and the growth rate is strongly decreased or even blocked. Adsorption can also occur on the surface with bonds so strong that impurity molecules cannot move and form a barrier through which the steps have to filter. The spreading of steps beyond this barrier demands supersaturation higher than a critical value for each impurity concentration. In this case impurities are incorporated with tailor-made additives that are used to modify the crystal habit for industrial needs. The molecules of these impurities are similar to those of crystals, but contain some structural differences, so that when they are incorporated into the crystal they disrupt some bonds and change the growth rate of the faces.

3. CLASSIFICATION OF CRYSTAL GROWTH

The methods of growing single crystals may be classified according to their phase transformation as follows:

- Growth from solid → solid-solid phase transformation.
- Growth from liquid → liquid-solid phase transformation.
- Growth from vapor → vapor-solid phase transformation.

One can consider the conversion of the polycrystalline piece of a material into a single crystal by imagining that the grain boundaries are swept through and pushed out of the crystal in the solid-solid growth of crystals. The crystal growth from liquid falls into four categories namely: 1) Melt growth, 2) flux growth, 3) hydrothermal growth, and 4) low-temperature solution growth.

There are number of growth methods in each category. Among the various methods of growing single crystals, solution growth at low temperature occupies a prominent place, owing to its versatility and simplicity.[41–43] Growth from solution occurs close to equilibrium conditions and hence crystals of high perfection can be grown.

4. LOW-TEMPERATURE SOLUTION GROWTH

Solution growth is the most widely used method for the growth of crystals when the starting materials are unstable or decompose at high temperatures. This method demands that the materials must crystallize from solution with prismatic morphology. In general, this method involves seeded growth from a saturated solution. The driving force, i.e. the supersaturation, is achieved either by temperature lowering or by solvent evaporation. This method is widely used to grow bulk crystals that have high solubility and a variation in solubility with temperature. After many modifications and refinements, the process of solution growth now yields good-quality crystals for a variety of applications. Growth of crystals from solution at room temperature has many advantages over other growth methods, though the rate of crystallization is slow. Since growth is carried out close to room temperature, the structural imperfections in solution grown crystals are relatively low.

4.1 Solution Growth Methods

Low-temperature solution growth can be subdivided into the following categories:

- Slow-cooling method.
- Slow-evaporation method.
- Temperature gradient method.
- Chemical/gel method.

4.1.1 Slow-Cooling Method

Slow cooling is the best way to grow crystals by solution technique. The main disadvantage of the slow-cooling method is the narrow range of temperature; hence, much of the solute remains in the solution at the end of the growth run. To compensate for this effect, a large volume of solution is required. A wide temperature range may not be desirable, because the properties of the grown crystal may vary with temperature. Even though this method has the technical difficulty of requiring a programmable temperature control, it is widely used with great success. In the slow-cooling method if growth occurs without any secondary nucleation in the solution, the supersaturation is fixed within the metastable zone limit. A large cooling rate changes the solubility beyond the metastable zone width and multinucleation occurs at the expense of the seed crystal. A balance between temperature lowering and the growth rate has to be maintained. Growth at a low super-saturation prevents strain and dislocation formation at the interface. Supersaturation can be increased after initial growth to arrive at a reasonable growth rate.

4.1.2 Slow-Evaporation Method

This method is similar to the slow-cooling method in terms of the apparatus requirements. The temperature is fixed and provision is made for evaporation. With nontoxic solvents, like water,

it is permissible to allow evaporation into the atmosphere. Typical growth conditions involve a temperature stabilization of about ± 0.05 °C and rates of evaporation of a few mm^3/hr. The evaporation technique has an advantage that the crystals grow at a fixed temperature. But inadequacies of the temperature control system still have a major effect on the growth rate. This method can effectively be used for materials having very low-temperature coefficient of solubility.

4.1.3 Temperature Gradient Method

This method involves the transport of materials from a hot region containing the solute material to be grown to a cooler region, where the solution is supersaturated and the crystal grows. The main advantages of this method are as follows:

- Crystal grows at a fixed temperature.
- Insensitivity to temperature changes, provided both the source and the growing crystal undergo the same change.
- Economy of solvent and solute.

On the other hand, a small temperature difference between the source and the crystal zones has a large effect on the growth rate.

4.1.4 Chemical/Gel Method

The gel method is exceedingly simple. One procedure is to prepare the gel using a commercial water glass adjusted to a specific gravity of 1.06 g/cm^3. Gel is then mixed with 1-M tartaric acid and allowed to gel in a test tube. Once the gel is formed, some other solution can be placed on the top (1M $CaCl_2$ solution) as shown in figure 3. In the due course of time, crystals of calcium tartrate tetrahydrate are formed in the gel. In a nutshell, one solution diffuses through the gel and reacts with the other solution to form crystals of appropriate chemicals.[44]

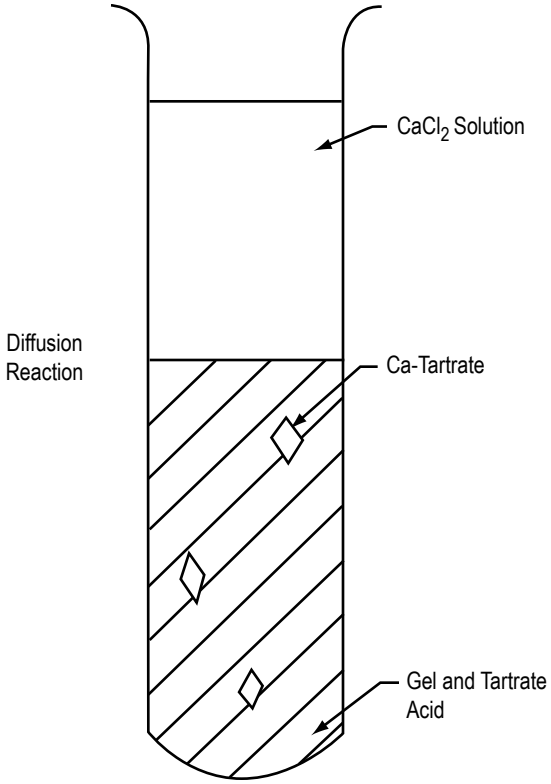

Figure 3. Schematic diagram of the gel crystal growth process.

5. SOLUTION GROWTH BY TEMPERATURE LOWERING

The growth of crystals from solution from low-temperature solutions occupies a prominent place, especially when materials are not stable at elevated temperatures. A number of concepts for solution crystal growth systems are found in literature. One of the best concepts for growth of both inorganic and organic crystals from solution is by temperature lowering of a solution, provided the material has a positive temperature coefficient of solubility. In this method, a saturated solution of the material to be grown, is prepared at a chosen temperature and kept at this temperature for 24 hr. Then, the seed-holding rod is inserted in the growth chamber and rotation is initiated. The growth process is initiated by slowly lowering the temperature. The temperature of the solution is lowered at a preprogrammed rate, typically 0.05 to 2 °C per day depending on the solubility of the chosen material. The complete crystallization process may take from a week to several weeks. To terminate the growth process, the grown crystals are taken out of the solution without thermal shock.

A solution crystal growth is a highly complex process and depends on various growth parameters such as seed quality, growth temperature, temperature lowering rate, solution character, seed rotation, and stirring of solution along with other conditions. To grow good-quality crystals, these parameters have to be optimized for each crystal.

5.1 Solvent Selection and Solubility

A solution is a homogeneous mixture of a solute in a solvent. The solute is the component present in a smaller quantity. For a given solute, there may be different solvents. Apart from high purity starting materials, solution growth requires a good solvent. The solvent must be chosen by the following factors taking into account:

- High solubility for the given solute.
- Good solubility gradient.
- Low viscosity.
- Low volatility.
- Low corrosion.

If the solubility is too high, it is difficult to grow bulk single crystals; and if too small, solubility restricts the size and growth rate of the crystals. Solubility data at various temperatures is essential to determine the level of supersaturation. Hence, the solubility of the solute in the chosen solvent must be determined before starting the growth process. If the solubility gradient is very small, slow evaporation of the solvent is the other option for crystal growth to maintain supersaturation in the solution. Crystal growth from solution is mainly a diffusion-controlled process; the medium must be less viscous to enable faster

transference of the growth units from the bulk solution to the growth site by diffusion. Hence, a solvent with less viscosity is preferable. Most importantly, single crystals such as potassium dihydrogen phosphate (KH_2PO_4) and (L)-arginine phosphate monohydrate (LAP) are grown in aqueous solutions, or in solvents that are mixtures of water and miscible organic solvents. Of all known substances, water was the first to be considered for use as a solvent because it is nontoxic, most abundant, and low cost. A proper choice of solvent, based on knowledge of its chemical reactivity, helps one to avoid undesired reactions between solute and solvent. Except that, in general, the solubility of the growth materials in solvents is required to be sufficiently large. The solubility parameter (δ) can often be used in estimating the solubility of non-electrolytes in organic solvents as follows:

$$\delta = (\Delta U/V_m)^{1/2} = (\Delta H - RT/V_m)^{1/2} \quad , \tag{15}$$

where V_m is the molar volume of the solvent, ΔU is the molar energy, and ΔH is the molar enthalpy. δ is a solvent property that measures the work necessary to separate the solvent molecules. Often a mixture of two solvents, one having a δ value higher than that of a solute and the other lower, is a better solvent than either of the two solvents separately.[45] A selection of δ-values is given in table 1.

Table 1. Solubility parameters (δ) of water and some organic solvents at 25 °C.

Solvent	δ (MPa$^{1/2}$)	Solvent	δ (MPa$^{1/2}$)
Water	47.9	Acetic acid	20.7
Methanol	29.6	1,4-Dioxane	20.5
Ethanol	26.0	Carbon disulfide	20.4
Formamide	39.3	Cyclohexanone	20.3
N-Methylformamide	32.9	Acetone	20.2
1,2-Ethanediol	29.9	1,2-Dichloroethane	20.0
Tetrahydrothiophene-l, 1-dioxide	27.4	Chlorobenzene	19.4
N,N-Dimethylformamide	24.8	Chloroform	19.0
Dimethyl sulfoxide	24.5	Benzene	18.8
Acetonitrile	24.3	Ethyl acetate	18.6
1-Butanol	23.3	Tetrahydrofuran	18.6
Cyclohexanol	23.3	Tetrachloromethane	17.6
Pyridine	21.9	Cyclohexane	16.8
t-Butanol	21.7	n-Hexane	14.9
Aniline	21.1	Perfluoro-n-heptane	11.9

Another property that may also be considered when selecting solvent for crystal growth is the dipole moments between the solute and solvent. Most typical organic solvents have a dipole moment less than about 3 debye. Therefore, in the case of a solute having a similar dipole moment value, a much wider choice of solvents is possible.

5.1.1 Solubility Determination

Solubility is an important parameter for low-temperature solution crystal growth. Before any solution growth technique can be applied, congruent or incongruent solubility must be determined and the absence of compound formation with pure or mixed solvents must be achieved. In the latter case, a special compositional and thermal regime will be necessary to crystallize the desired phase. A simple apparatus for solubility studies is shown in figure 4. Visual inspection allows the solubility determination. Upon cooling, crystallized material is obtained for solid-phase analysis. This apparatus is easily fabricated and is very convenient for measuring solubility. The following is a brief description of how this has been achieved: The solute and solvent were weighed into a glass ampoule. The ampoule was seated and rotated in a bath controlled by a thermostat. The temperature was increased in steps of 0.5 °C every 1–2 hr. The final disappearance of the solute yields the saturation temperature. The accuracy of this measurement was within ±0.5 °C.

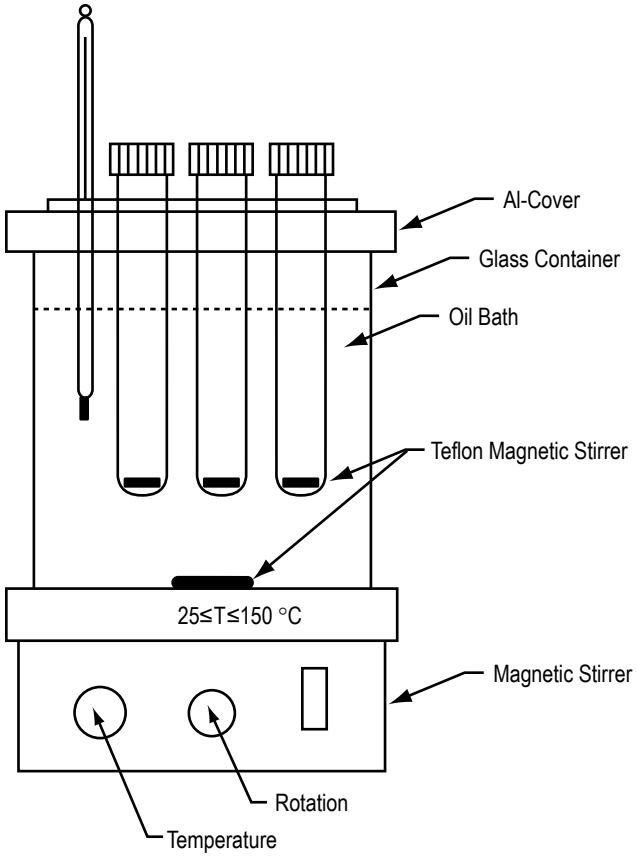

Figure 4. Apparatus for solubility studies as well as equilibration of feed material and growth solution.

The time needed to reach equilibrium for most covalent organic materials is usually shorter than that of sparingly soluble salts, but the settling times before analyses may be longer. In many soluble salts, such as KDP—KH_2PO_4, TGS—$NH_2CH_2COOH)_3H_2SO_4$, and ethylene diamine tetra acetic (EDTA)

acid—$C_{10}H_{16}N_2O_8$, the solubility is strongly temperature dependent. On the other hand, for some soluble salts, such as $LiIO_3$ and $Li_2SO_4H_2O$, the solubility is not dependent on temperature, and even has inverse slope.

Various techniques for measuring the solubility, such as methods based on the vortex flow caused by concentration and optical effects, can be found in the literature; however, an accurate measurement of

supersaturation is usually difficult. Some new methods such as holographic phase contrast interferometric microphotography and trace fluorescent probe have been developed. Using these techniques, concentration distributions and the thickness of boundary layers under different convection conditions can be measured with greater accuracy. Although these methods still need more development and refinement to become more generally applicable, they are promising alternatives for supersaturation determination of easily soluble compounds. Of course, if the solubility is known, supersaturation can be calculated by measuring the solution temperature and its equilibrium temperature. The problem is that equilibrium temperature measurements are not always easy.

5.2 Design of a Crystallizer

When designing a crystallizer for growing crystals from solution by the temperature lowering method, the following conditions should be met:[43,46–47]

- Range of operating temperature from room temperature to 80 ºC, depending on the solvent.
- Choice of hydrodynamic conditions in the solution.
- Measurement of growth parameters, such as growth rate.
- Arrangement for taking the grown crystals out of the crystallizer without any thermal shock.
- Arrangement for changing the saturation/temperature decrease rate.
- Possibility of changing the different kind of seed holders.
- Long-term operating reliability of the system.

Since these types of solution crystallizers are not available in the commercial market, the system must be designed and fabricated based on the particular requirements. The following is a brief description of a modified crystallizer for growing large crystals from solutions, along with the design of a versatile electronic reciprocating control system to change and reciprocate the motor speed containing the seed-holding rod.

An electronic system that allows the rotation rate and the number of clockwise and counter clockwise revolutions to be adjusted as desired. This system alleviates the jerky motion problem of the seed holder during reciprocation, as in earlier electromechanical systems designed by the authors.[48] Good-quality crystals of important nonlinear optical materials such as Methyl-(2,4-dintropheny)-aminopropanoate: 2-Methyl-4-nitroaniline (MNA:MAP), LAP, L-Histidine tetrafluoroborate (LHFB), L-Arginine

tetrafluoroborate (LAFB), and others such as TGS and KDP have successfully been grown in the authors' laboratory using this system.[47–58] The complete crystallization apparatus along with the electronic circuit can be easily fabricated in the laboratory with readily available components.

5.2.1 A Typical Solution Crystal Growth Crystallizer

A schematic diagram of a modified solution crystal growth system that the authors designed and fabricated in our laboratory, after designing a number of crystallizers, is shown in figure 5.[51] It consists of a 250-ml crystallizer jar (4), which holds the growth solution, that is placed inside a 2.5-L glass-jacketed kettle (2). The linear and reciprocating motion of the Teflon® seed holder (5) is controlled by a rack pinion arrangement (8) and electronic circuit (7). A reversible motor (6) is used for rotating the seed holder. The temperature of the growth solution is controlled and programmed by circulating water using a NesLab bath (1). To prevent evaporation of the solvent, a specially designed oil Teflon seal (3) and/or RTV/Teflon seal (3) are used.

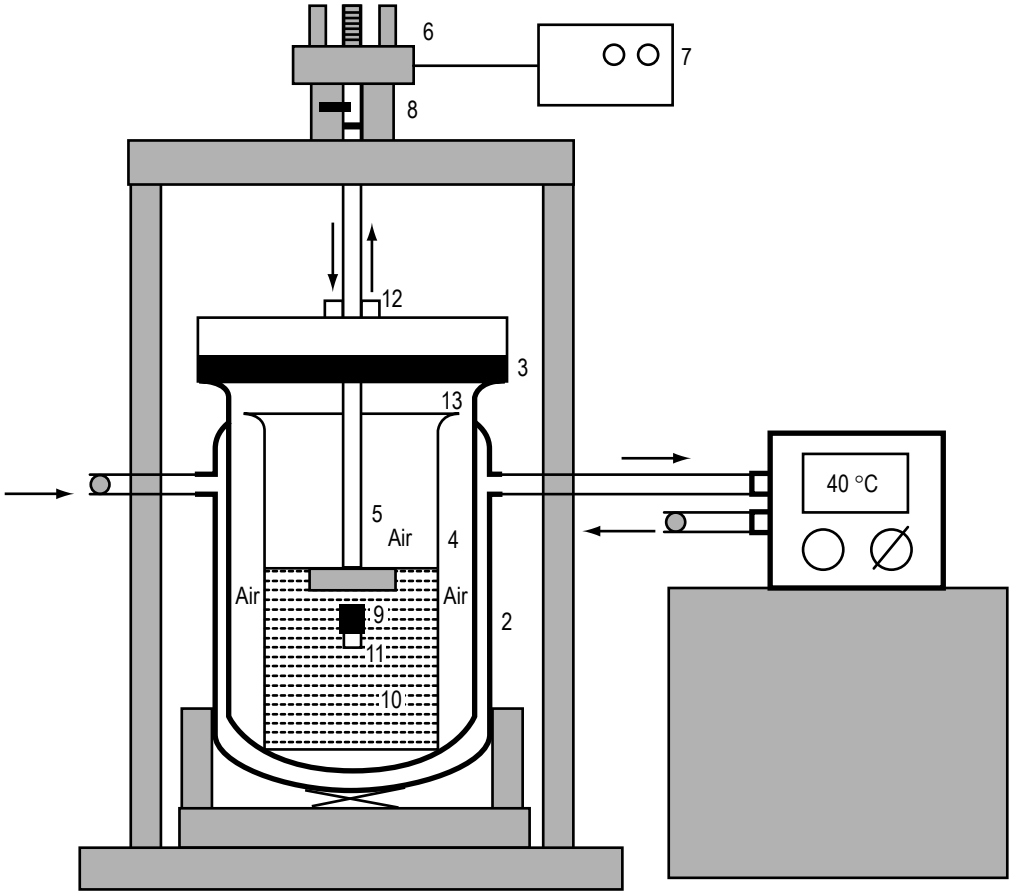

Figure 5. Schematic diagram of a new type of crystallizer for growing organic crystals with the following system components: (1) Circulating bath, (2) jacketed reaction kettle, (3) RTV/Teflon seal, (4) crystallizer jar, (5) Teflon seed holder, (6) reversible motor, (7) circuit for reciprocating and controlling the stirring rate of seed holder, (8) arrangement for pulling the crystal during growth, (9) Teflon tape cover, (10) solution, (11) seed crystal, (12) Teflon seal, and (13) glass lid.

The main advantages of this crystal growth system are:

- Better temperature stability, even with sudden fluctuations in room temperature.
- Better control over organic solvent evaporation.
- A mechanical screw type arrangement for pulling the seed crystal at a controlled rate.
- The possibility of varying the seed orientation and type.
- A versatile electronic reciprocating control system to change and reciprocate the motor speed containing the seed-holding rod.

Better temperature stability was accomplished by loading the growth solution in a beaker kept inside the jacketed vessel. An air gap provides extra insulation. Moreover, spontaneous nucleation at the bottom of the growth vessel, which hampers growth and the crystal yield, is completely eliminated. By providing an extra lid on the inside beaker and a Teflon seal over the jacketed vessel, evaporation of the solvent was reduced dramatically. The inner beaker is filled halfway with solution rather than three-fourths, as usually done, and the growing crystal is pulled in a controlled fashion. Since filling the inner beaker to three-fourths is not required, the crystal is annealed in situ and the spurious aloe vera treelike growth, near the seed in some crystals such as MNA:MAP, is greatly reduced or completely eliminated.

Figure 6 (a) shows the seed crystal, along with an MNA:MAP crystal, grown using the usual technique, without pulling the growing crystal. Figure 6 (b) shows the same crystal grown with pulling, where the aloe vera treelike growth is avoided. Furthermore, when the crystal is pulled while growing, large crystals can be grown from a smaller amount of expensive mother liquor.

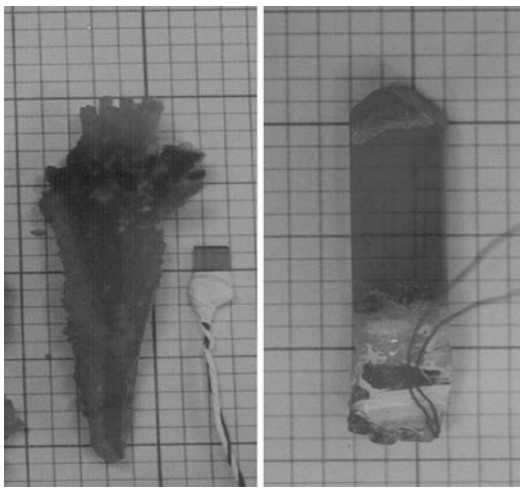

Figure 6. MNA:MAP seed (a) with aloe vera treelike growth and (b) without aloe vera treelike growth.

Figure 7 is a three-dimensional cutout view of another modified solution growth crystallizer with recipro-cating seed arrangement and other components that was also designed in our laboratory. It uses a magnetic stirrer to keep the temperature of the water bath uniform at a particular temperature. A layer of silicon oil on the surface of the water was found to reduce the water evaporation to a minimum, which is a big improvement over earlier designs.

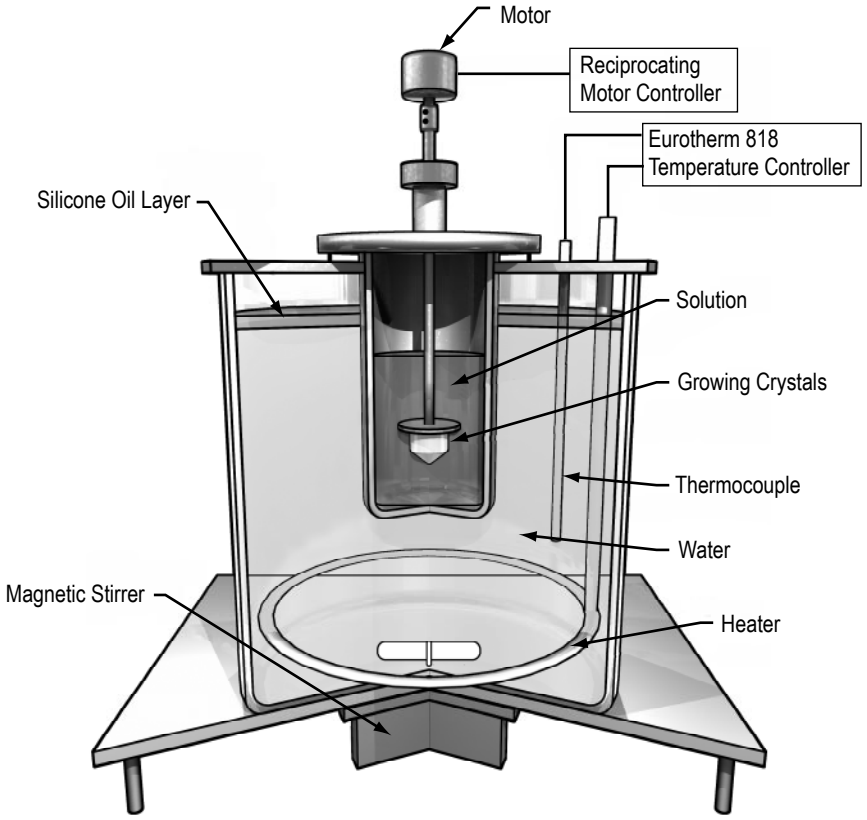

Figure 7. Modified crystallizer with arrangement to stop water evaporation.

Besides temperature control, the uniform rotation of seeds is required so stagnant regions or recirculating flows are not produced; otherwise, inclusions in the crystals will be formed. To study and achieve uniform and optimum transport of solute to the growing crystals, various seed rotation mechanisms have been used in the past. The unidirectional seed rotation leads to the formation of cavities in central regions of a crystal face, because of lesser solute transport to this region than to the edges and corners of the growing crystal. Furthermore, nonuniform solute supply favors the formation of thick layers that subsequently lead to the trapping of inclusions and the generation of dislocations. Periodic rotation of the growing crystal in opposite directions suppresses edge formation, but does not eliminate the formation of the central cavity. To avoid these defects and stagnant regions in the solution, an eccentric or clockwise and counter clockwise motion of the seed holder is used in growing crystals from solutions. A few mechanisms have been used in the past to generate the reciprocating motion of the seed holder

such as electromechanical and rack-pinion.[54–56] In the electromechanical system, a connection of the motor polarity is mechanically reversed by using a microswitch. There is a jerky motion on reversal in this mechanical system that sometimes causes seeds to fall down. The jerky motion also creates a turbulent flow in the fluid and a nonuniform transfer of solute to the growing faces, thereby defective crystals may be formed. The microswitch has to be changed frequently due to mechanical failure. Furthermore, the effect of seed rotation rates on the growth rate and the quality of the crystals cannot be systematically studied because rotation rate cannot be varied. In the rack-pinion arrangement, there is no jerking motion but one has to change gears to change rotation and reversal rate, which is quite an involved process.

To improve on these drawbacks, a versatile solid-state electronic circuit for reciprocating the direction of the seed holder was designed in our Crystal Growth Laboratory at Alabama A&M University, with added features to vary rotation rate, stopping time on reversal, and controlled timing for clockwise and counter clockwise motion of the crystal/seed holder.[57] These design features will allow crystal growers to more decisively study the effect of seed rotation rates on the growth and quality of the grown crystals, thereby optimizing this important parameter for growing better quality crystals.

A schematic diagram of the basic electronic circuit for the reciprocating motion control is shown in figure 8. The timer (Chip LM 555, U3) produces a square-wave timing pulse. It may be set for a particular frequency (POT1) and duty cycle (POT2) in combination with the timing capacitor (C3), and reset by the switch (S2) if necessary. The timing-wave form is divided by the J–K, 74LS112, flip-flop chip (U1) to one half the timer frequency. Parasitic oscillations are suppressed by capacitors (C1, C2, and C4). The two wave forms are combined by NAND gate chips SN7400 (U2) to alternately turn on the transistor (Q1 and Q2) to control the solid-state relays (1 and 2) that connect the alternate sides of the motor capacitor to the 110 VAC return line. Similarly, the transistors (Q3 and Q4) alternately turn on the indicator lamps (LED1 and LED2). Resistors (R1–R8) provide current limiting and bias. Motor rotation speed is controlled by the potentiometer (POT3). A power supply, consisting of the step-down transformer (T1), voltage regulator (U4) and associated filtering circuit (D1 and D2, C5 and C5), and voltage setting divider (R9 and R10) provides 5 VDC to the circuit. The operation of the circuit causes the following sequence of states in the system:

- First interval.
  - Seed holder motor runs counter clockwise.
- Second interval.
  - Motor comes to a stop.
- Third interval.
  - Motor runs clock wise.
- Fourth interval.
  - Motor again comes to stop.

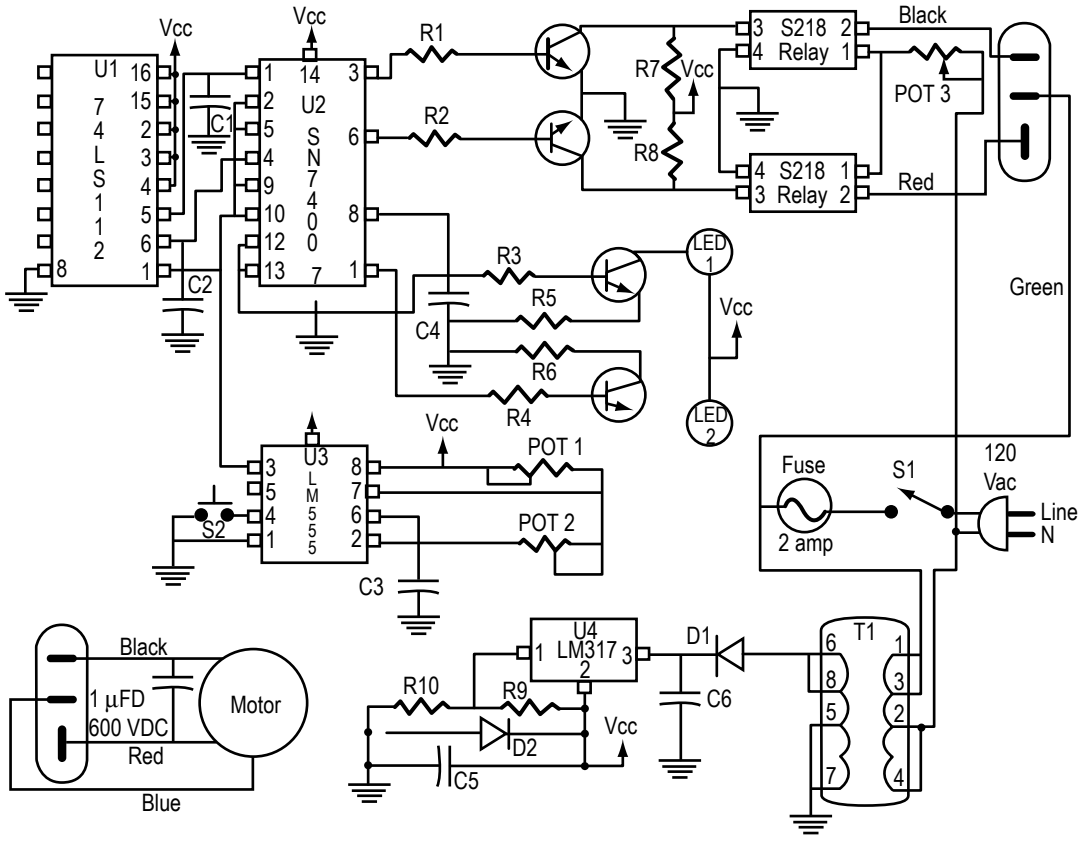

Figure 8. Solution crystallizer electronic circuit diagram for the reciprocating motion of the seed holder.

Then the entire cycle of operation is repeated and the intervals can be varied, as needed, for a particular crystal growth experiment.

5.2.2 Crystal Seed Holder

To ensure the best growth conditions, it is necessary to use a special crystal holder because the success of an experiment may depend upon its suitability. The selection of the crystal holder and the method for attaching a seed to it are no less important than the selection of the growth method. A crystal holder should ensure that a seed is held securely in a desired orientation and that the seed, and therefore the growing crystal, can be moved in any required manner. Also, the crystal holder should not become deformed at the selected speed, motion direction, or weight of the final crystal grown on it. The crystal holder material should be chemically inert in the solution of the substance being crystallized.

Two Plexiglas® seed holders, shown in the schematic diagram in figure 9, were specially designed, fabricated, and used successfully by the authors for aqueous solution crystal growth.

5.2.3 Preparation of the Seed Crystal and Mounting

A seed is small fragment of a crystal or a whole crystal that is used to start the growth of a larger crystal in a solution. This seed must meet the following requirements:

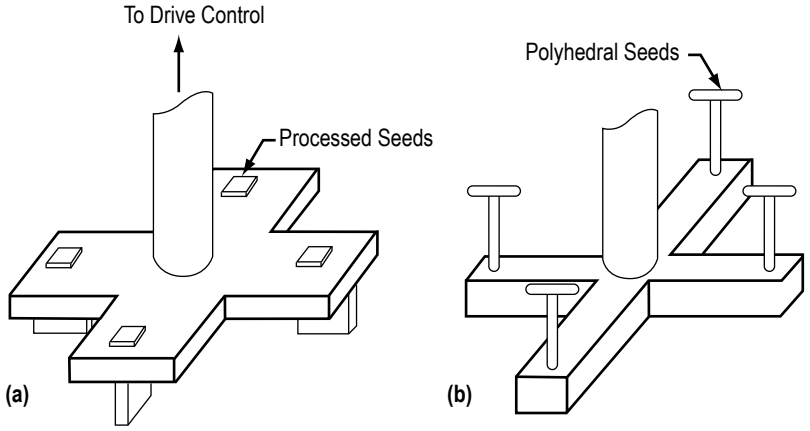

Figure 9. Plexiglas seed holders for solution growth crystallizers.

- It should be a single crystal free of cracks or boundaries.
- It should be free of inclusions.
- Its surface should be free of any sharp cleaved edges.
- It must be grown under the same conditions as those to be used in growing the desired single crystals.

Following the requirements in preparing the seed crystals will result in the growth of high-quality crystals, provided other criteria such as solution preparation, etc. are performed carefully as well. Prior to crystal growth, seed crystals are mounted on Plexiglas rods using 100-percent silicon rubber Dow Corning Silastic 732 RTV adhesive.

5.3 Solution Preparation and Starting a Growth Run

It is essential to have the solubility data of the growth material at different temperatures for solution preparation. Sintered glass filters of different pore sizes are used for solution filtration. The clear solution, saturated at the desired temperature, is poured into the growth vessel. For growth by slow cooling, the vessel is sealed to prevent solvent evaporation. Before starting the crystal growth process, a small crystal suspended in the solution is used to test the saturation. By varying the temperature, a situation is obtained where neither growth nor dissolution occurs. The test seed is replaced with a good-quality seed. All unwanted nuclei and surface damage on the seed are removed by dissolving at a temperature above the saturation point. Growth is initiated after lowering the temperature to the equilibrium saturation. A controlled solvent evaporation can also be used in initiating growth. The quality of the grown crystal depends on the nature of the seed, cooling rate employed, and agitation of the solution.

Various new nonlinear optical crystals hold promise for use in optical processing devices such as LAP, LHFB, LAFB, MAP:MNA, and L-pyroglutamic acid have been successfully grown using the reciprocating system, previously described, in combination with the temperature lowering technique described by the authors.[47–50] Some of these crystals are shown in figure 10. In the investigators'

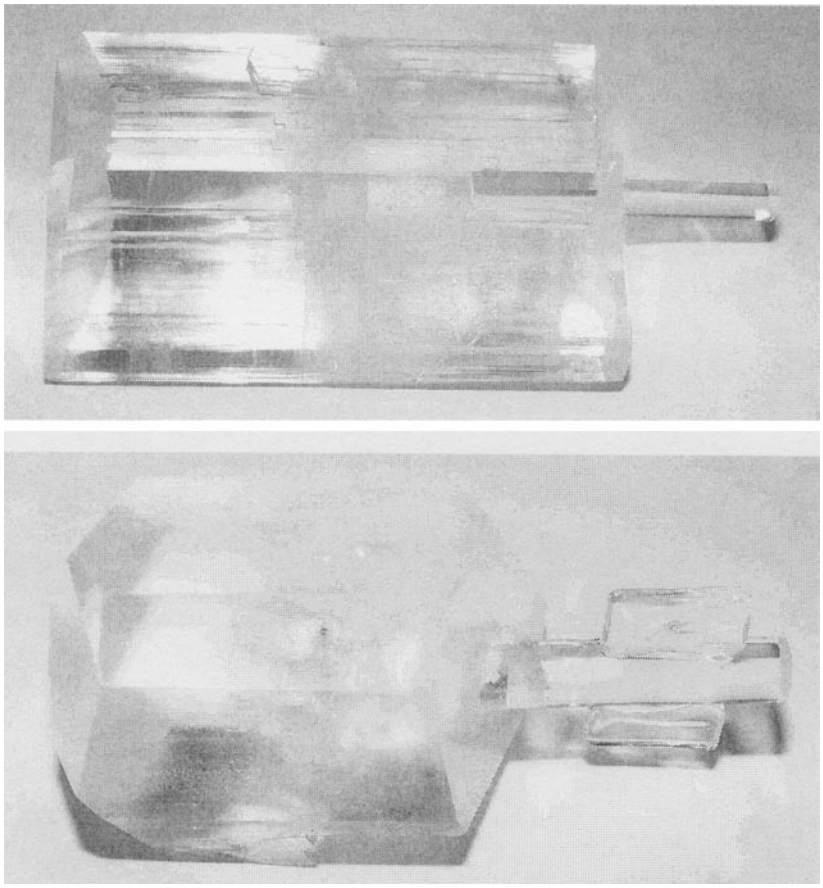

Figure 10. Photograph of crystals grown at Alabama A&M University (a) LHFB and (b) L-pyroglutamic acid crystals.

observation and experience, there is significant improvement in the quality of grown crystals and the success rates of the growth runs, which is evident from the transparency and less scattering that is observed using laser illumination. This reciprocal motion control electronic system for solution growth crystallizers has been in use in our laboratory for several years and continues working satisfactorily.

It is worthwhile to mention that this simple and versatile crystallization apparatus can be fabricated in any college, university, or scientific laboratory from readily available components. Besides its use in physics or chemistry laboratory experiments, it can also be used for extensive research on the effect of important parameters such as seed rotation rate, reversal stopping time, and number of rotations in the clockwise or counter clockwise direction on the quality and growth rate of technologically important crystals.

6. TRIGLYCINE SULFATE CRYSTAL GROWTH—A CASE STUDY

TGS is one of the most important ferroelectric materials. The ferroelectric nature of TGS, $(NH_2CH_2COOH)_3H_2SO_4$, was discovered by Matthias, Miller, and Remeika and discussed by Jana and Shirane.[59] The TGS crystal structure was reported by Hoshino, Okaya, and Pepinsky. In the ferroelectric phase below the Curie temperature ($Tc \approx 49$ °C), the symmetry is monoclinic with space group $P2_1$. Above the Curie temperature, the structure gains an additional set of mirror planes in the space group $P2_{1/m}$. It has been reported that $a = 9.42$ Å, $b = 12.64$ Å; $c = 5.73$ Å; $\beta = 110°23'$ and that the structure contains three independent glycine molecules. One of the structures, designated as glycine II, has a zwitter-ion configuration $(NH_3)^+CH_2OO^-$ and the other two $(NH_3)^+CH_2COOH$. The TGS may be called glycine-diglycinium sulfate with chemical formula $((NH_3)^+CH_2COO^-).((NH_3^+)CH_2COOH)_2.SO_4^{2-}$. The projection of the structure along the *c*-direction is illustrated in figure 11. Glycine I deviates only slightly from the plane *m'* at $y = ¼$ on which the $[SO_4]^{2-}$ tetrahedra also lie, whereas glycine II and III are approximately related by inversion through (½,½,½).[60]

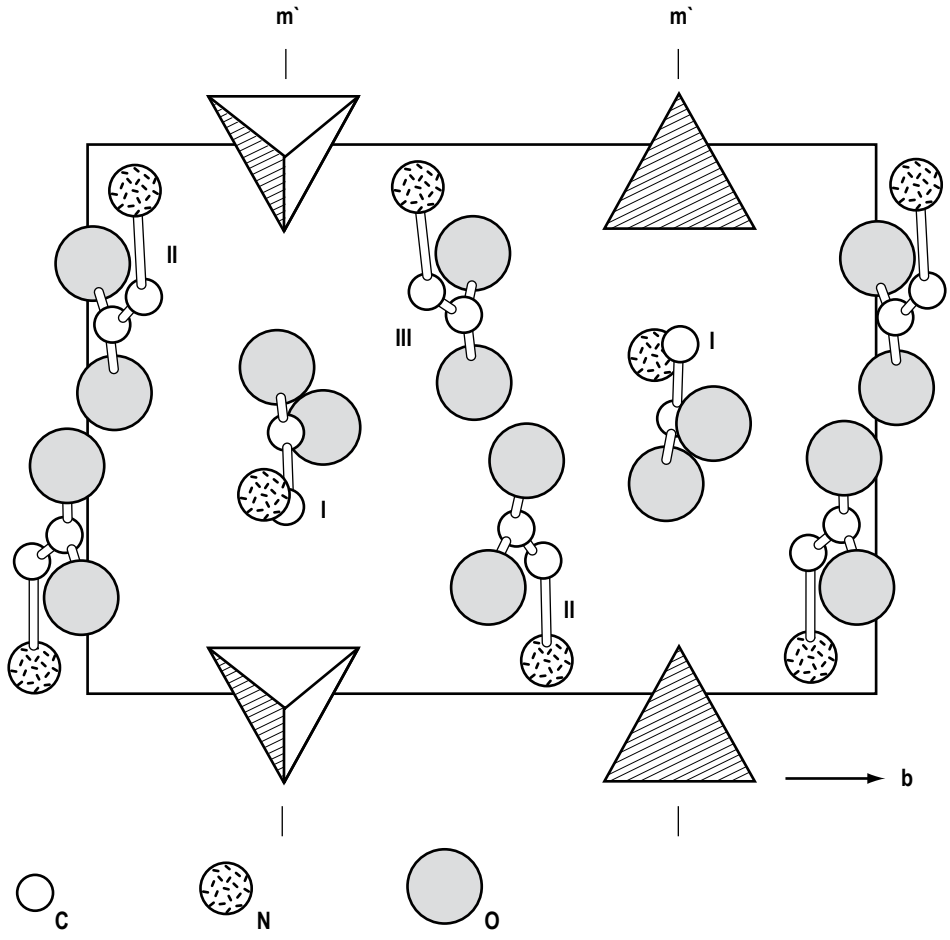

Figure 11. Projection of the TGS crystal structure along the *c*-direction: *ṁ* represents the set of pseudo-mirror planes in which glycine-I molecules are inverted on ferroelectric switching.

6.1 Growth of Triglycine Sulfate Single Crystals

Single TGS crystals have usually been grown from aqueous solution by the temperature lowering or solvent evaporation method. The authors have successfully grown TGS crystals using the crystallizer, illustrated by the schematic diagram shown in figure 12.[58] The outside water bath with a capacity of about 12 liters, and the inside smaller cubical growth cell with a 1-liter capacity were made out of Plexiglas. Crystallizer temperature control is achieved using a 250-W immersion heater controlled by YSI 72 proportional temperature controllers to an accuracy of ± 0.1 °C. Uniformity of the temperature throughout the bath is achieved with the help of a fluid circulation pump. The bath temperature is monitored at two points during the crystal growth using NBS calibrated thermometers. The crystals are grown by slowly cooling the solution at any desired rate.

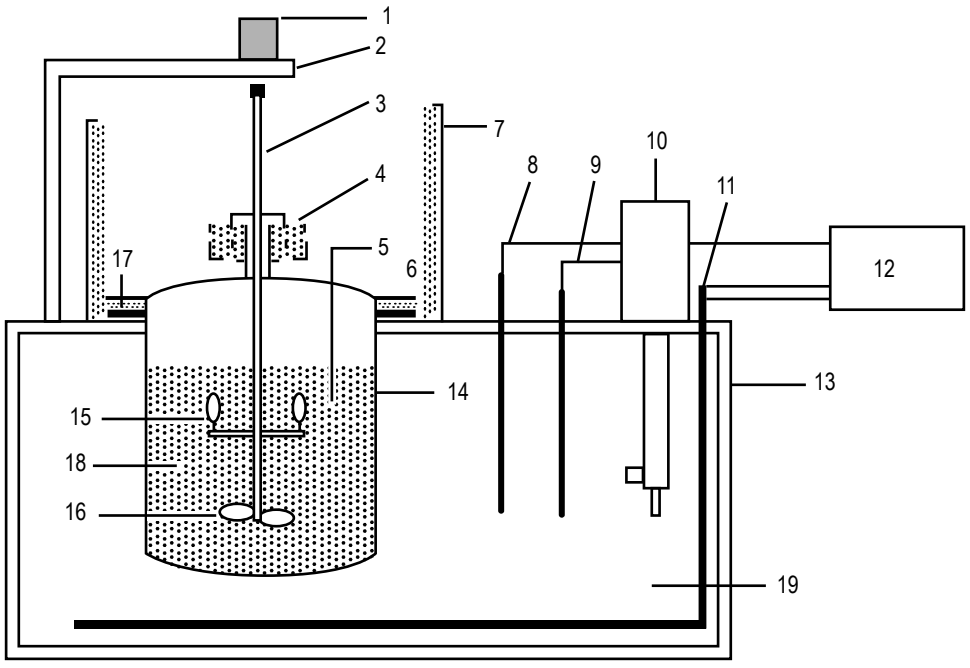

1. Reciprocating Motor
2. Motor Mounting Stand
3. Seed Mounting Glass Rod
4. Seal to Limit Evaporation
5. Glass Thermometer
6. Air-tight Class Cover
7. Post-Growth Anealing Heater
8. Control Thermister
9. Recording Thermister
10. Fluid Circulation Pump
11. Water Heater
12. Temperature Controller/Programmer
13. Plexiglass Water Bath
14. Pyrex Crystal Growig Cell
15. Seed/Crystal
16. Stirrer Blades
17. Teflon Gasket
18. Solution
19. Water

Figure 12. Reciprocating motion crystallizer schematic diagram.

TGS crystals are doped with L-alanine to enhance performance and check depoling for their use in infrared sensor element. A rotating disc technique has been applied to grow uniformly L-alanine-doped TGS crystals using a large-area seed crystal having a large (010) face.[61] A conventional crystallizer was modified to allow growth under suitable hydrodynamic conditions to stabilize growth on the (010) face. Such a crystallizer is shown in figure 13. In this crystallizer, a seed crystal in the form of a disc was held in a circular holder with the (010) face exposed to the solution. The disc was attached to the end of

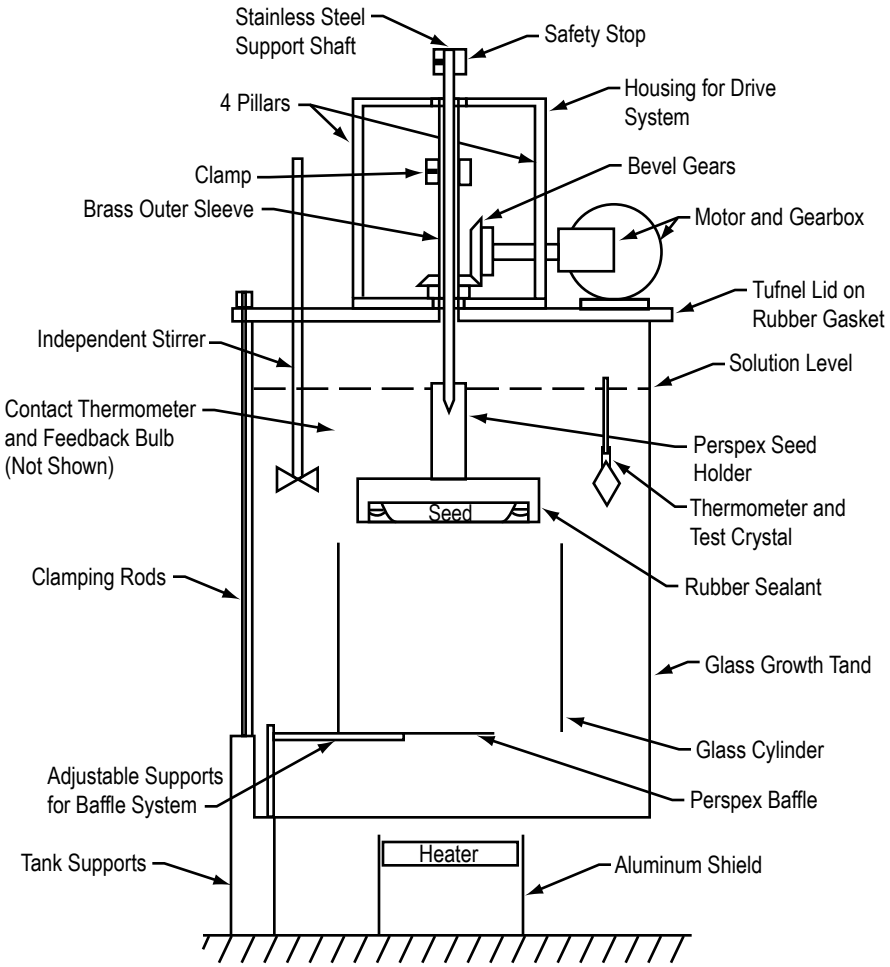

Figure 13. Apparatus for spinning disc growth.

a spindle that was rotated at 340 rpm. This creates a uniform boundary layer of solution over the crystal's exposed face. The container with a 30-liter capacity was heated by a hot plate spaced from its bottom surface and regulated to hold the temperature with in ±0.01 ºC. The solution rises from the bottom of the vessel but hotter liquid is prevented from reaching the crystal directly by a Plexiglas baffle. A growth rate of 1 mm/day was maintained by lowering the temperature uniformity at 0.05 ºC/day. The resulting crystals propagating from the seed were found visibly to be of good quality without defects. In addition to uniform doping and the growth of high-quality crystal, this method has several other useful features such as short growth time, with decrease cost and reuse of seeds, and growth occurs within a small temperature range. Brezina, et al. designed a crystallizer for growing L-alanine-doped deuterated triglycine sulfate (DTGS) crystals by isothermal evaporation of D_2O.[62] Satapathy, et al. have described a novel technique for mounting the TGS seeds and a crystallizer.[63] Banan has also described a crystallizer and a seed holder for growing pure and doped TGS crystals.[64]

TGS crystals weighing more than 100 grams have been grown from solution with ethyl alcohol additions.[65] When alcohol is mixed in an aqueous solution of TGS, part of the water in the solution associates with alcohol, which concentrates the solution. Thus, supersaturation can be controlled to a certain degree, making it easier to grow TGS crystals.

To achieve success in growing crystals from aqueous solutions, it is important to prepare a solution with a well-determined saturation temperature, solubility profile, and absence of any foreign particles. For our investigation, TGS solution was prepared using high-purity crystalline TGS by BDH, UK. The solubility of TGS at various temperatures were determined and compared with information available from various sources. TGS solution was prepared at 40 ºC saturation temperature. To prepare saturated solution, 464 grams of TGS was weighed and dissolved in 1,000 cc of distilled water. The mixture was heated to 50 ºC and mixed thoroughly using a Teflon coated magnetic stirrer. The solution was then filtered through a 5-micron filter funnel using a vacuum unit. After filtration, this solution was transferred into the growth chamber. To start the growth run, the bath temperature was kept at 45 ºC. The solution was poured into the growth cell. The temperature was then reduced to 41.5 ºC, 1.5 degree above the saturation temperature, and was allowed to stabilize overnight. The saturation temperature was again checked by crystal insertion into the solution technique, and also refractive index measurements. For each saturation point, the refractive index was measured at different temperatures before hand using an Abbe refractometer. The starting growth temperature was adjusted based on the result of this procedure. After this, the seed-crystal holder was placed in an oven and heated to 45 ºC. All precautions were taken to keep the seeds, as well as the holder surface, free of dust or foreign particles prior to transferring to the growth cell. The preheated seed-crystal holder was then inserted into the growth cell and the holder was attached to the reciprocating apparatus. The seed crystals were slightly dissolved and the growth run started. The bath temperature was reduced by 0.1 ºC/day initially, and at the final stage of growth by 0.2 ºC/day. Removal of the grown crystals from the mother liquor requires some care. Mishandling may induce defects, thus destroying the scientific value of the crystal or even fracture it all together. To avoid cracking the crystals, due to thermal shock, the crystals were wrapped in a lint-free paper towel maintained at final growth temperature. The crystals were then transferred to an oven kept at an appropriate temperature. The temperature of the oven was slowly lowered to room temperature. Since RTV 732 adhesive was used for mounting the seed crystal, the grown crystals can be easily removed from the seed holder by the fingers using slight force.

6.2. Growth Kinetics and Habit Modification

TGS normally grows with the habit shown in figure 14. It is observed that the growth rate $V_{(010)}$ is much faster than $V_{(001)}$. So the (010) face, as seen in figure 14 is very small or not present. Both the growth kinetics and habit modifications of TGS have been extensively studied over the past several decades. The work published so far has resulted in a description sufficient for reliable growth of this crystal as described previously. A number of studies of TGS growth kinetics grown from aqueous solution have been reported in the literature.[66–71] Novotny and Moravec studied the growth of the (110) face of TGS crystals grown isothermally above the phase transition, at higher supersaturation ($\sigma > 10^{-3}$) and under constant hydrodynamically controlled conditions.[69] The researchers observed that the ratio of growth rates along the individual axes is $V_a:V_b:V_C$=0.67:1:0.25. On the basis of the measured dependence of the linear growth rate upon supersaturation (σ), it was found that the growth of the (110) face is probably controlled by volume diffusion of TGS molecules toward the surface of the growing crystal. Increasing supersaturation caused a reduction of the number of faces in the prismatic zone of the crystal and an increase of the dislocation density in the (110) faces. Measurements of the (110) and (001) faces growth rates, as a function of supersaturation of the solution, were also analyzed on the basis of the surface-diffusion model of Burton, Cabrera, and Frank (BCF).[69,67] It was shown that surface diffusion is responsible for

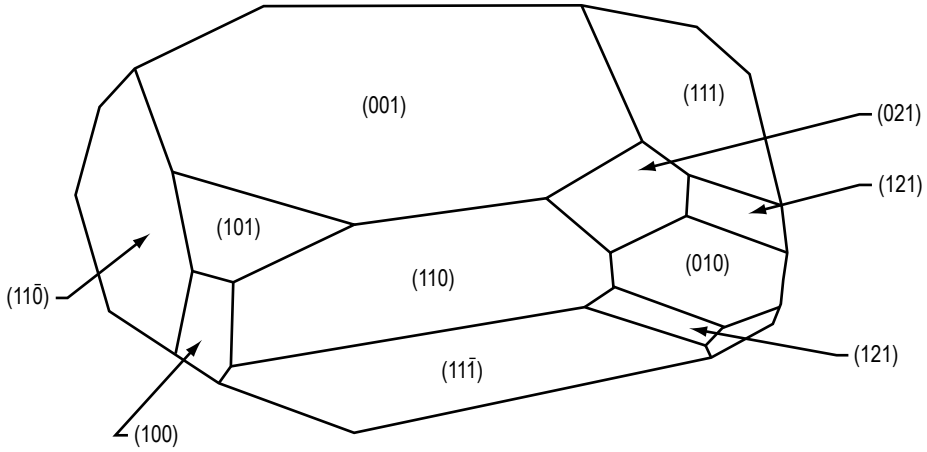

Figure 14. Normal growth habit of TGS crystal.

the low-growth rates of (001) faces; but in the case of (110) faces, the mechanism is less important at higher values of supersaturation than volume diffusion. Rashkovich investigated the growth of (001) faces below the transition temperature.[68] The results were qualitatively consistent with the dislocation model of crystal growth, but growth at low supersaturation did not agree with the BCF model.[67]

Reiss, et al. studied the growth of crystals at 33.55 °C at relative supersaturations of 0.004 and 0.045.[71] In their study, both BCF and birth of spreading growth laws are fitted to the growth rate data. They also found that qualitative aspects of the growth are consistent with the BCF model.

The role of pH, impurities, degree of supersaturation, growth temperature, and technical parameters including seed preparation, attachment, etc. on growth kinetics has also been quantitatively investigated by various investigators.[72–90] The results are described in section 6.2.1.

6.2.1 Effect of Seed Crystal

It has been observed that morphology does not change much for seed crystals obtained at different temperatures.[79] However, at higher temperatures (35–45 °C) seeds tend to be elongated in the (001) direction, while seeds grown at lower temperatures are nearly isometric. Morphological study of the crystals grown using the previously cited seeds, showed the dependency of the crystal habit on the characteristics of the seed. The grown crystals tended to be elongated when the elongated seeds were used. Crystals with large-sized (010) faces grew when cleaved platelets were used for seeding. Crystals with high transparency and lower dislocation densities were obtained when the crystal growth temp-erature was kept the same as that used to grow the seed. Crystal growth was seriously impaired when cleaved platelets were used as seeds, because of unwanted nucleation that started growing during the growth process. Banan, et al. studied the effect of using poled seed on the morphology and growth rate of TGS crystals.[81] Table 2 summarizes the normalized growth data for two crystal growth runs using poled and unpoled seeds and figure 15 gives the morphology of the resulting TGS crystals. A number of interesting effects on the growth rate and morphology of these crystals were observed. Generally, the growth rate along the (010) $-b$ axis was faster than along (010) $+b$ axis. The well developed (010)/(0$\bar{1}$0) faces, which are generally not present or less developed in pure TGS crystals, were prominent and large in crystals

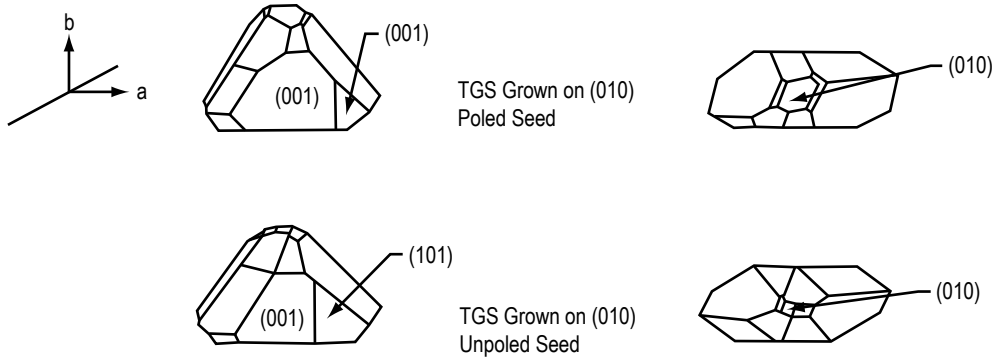

Figure 15. Growth habits of TGS crystals grown on (a) poled and (b) unpoled seeds.

grown on poled seed. In this way, identification of the ferroelectric axis in the TGS crystal becomes easier, and cleaving normal to the ferroelectric axis for preparation of pyroelectric IR element can be economically accomplished. It can be inferred from table 2 that growth velocity along the (010) axis of TGS crystal is affected by using a poled seed crystal. The decrease in growth rate along the (010) direction, in the case of poled seed, helps in the emergence of larger (010) faces.

Table 2. Crystal growth data for TGS crystals grown on poled and unpoled seeds.

TGS Crystals	Crystal Yield wt (g/day °C)	Growth Velocity, $V_{(010)}$ (mm/day °C)
(010) poled seed	0.618	1.05
(010) unpoled seed	0.621	1.16
(010) poled seed	0.624	1.20
(010) unpoled seed	0.637	1.25

6.2.2 Effect of Growth Temperature and Supersaturation

The dependency of crystal morphology and quality on growth temperature using seed obtained from the growth solution and at the crystal growth temperature has also been studied.[79] The change in morphology was not substantial, but the rate of growth in different directions changed with the temperature and relative change in the size of the faces was observed. Extra nuclei hindered the growth at higher temperature (40 °C) and the crystals were of poor quality with low transparency. The change in habit of TGS crystals as a function of temperature and supersaturation is shown in figure 16.[75]

6.2.3 Effect of pH on the Solution

The influence of solution pH on the growth, morphology, and quality of TGS crystals has been studied by a number of workers. It was observed that crystal quality is not affected much by pH variation.[79] The influence of growth solution pH on growth rates of various faces (001, 010, 100) and TGS habit was studied by Tsedrik, et al.[75]

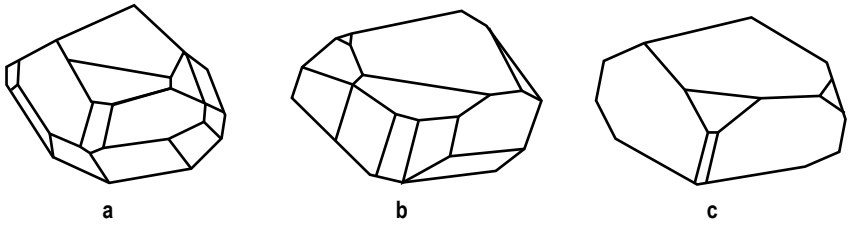

Figure 16. Change of TGS growth habits with growth temperature and supersaturation (a) 32 °C/0.7×10^{-3}, (b) 32 °C/3×10^{-3}, and (c) 52 °C/3×10^{-3}.

At a pH <1, diglycine sulfate (DGS) was formed. Table 3 gives the values of average growth rate (V) of (001), (010), and (100) faces of TGS crystals versus pH of the solution, as well as DGS grown at pH 0.3. Values for V(100) decreased monotonously with the lowering of pH and V(001) and V(100) had a local minima near the pH value corresponding to the stoichiometric (pH=2.14) value and a local maxima around pH=1.25. The crystal habit is defined by the growth rates of the faces. Figure 17 shows the dependence of crystal habit on pH.[75] The most isometric crystals were obtained at pH=1.55, when V (100/001) ≈1 (fig. 17 (c)). Almost all crystals at low pH had gaps on the (111) and (111) faces (fig. 17 (d) and (e)). These observed changes in morphology of TGS single crystals with the pH of the solution were apparently affected by different capture of incidental impurities, which are always present in the solutions. Chemical (structural) impurities captured with the crystal faces reduced the growth rates of the corresponding faces and mechanical impurities (defects) increased the rates. At low pH values, chemical impurities played the predominant role. Their entry into the growing crystal was increased with reducing pH. Table 3 clearly shows that the growth rate of all faces decreased with reducing pH, starting with pH=1.25. The gaps on (111) and ($1\bar{1}1$) faces were connected with strong hindering of the growth layers by the absorbed impurities (fig. 17 (d) and 17(e)). At high pH (>2), another kind of impurity (mechanical defect) has a predominant influence on crystal morphology. Their entry increased with rising pH, so the growth rates of all faces increased (table 3). At pH=1.55 the action of impurities of both kinds was comparable, and mostly isometric crystals were formed (figure 17(c)). Recently, it has been shown that the growth rate of the TGS and ATGSP (010) face crystals varies with the pH of the solution.[91]

Table 3. Growth rates of various faces of TGS versus pH of solution.[75]

pH	$V_{(001)}$ (10^{-3} mm/hr)	$V_{(010)}$ (10^{-3} mm/hr)	$V_{(100)}$ (10^{-3} mm/hr)
2.70	71.6	291.5	260.9
2.14	49.6	118.2	117.6
1.25	207.0	262.0	109.0
1.00	144.6	156.2	43.9
0.30	109.9	120.9	40.5

With the same supersaturation, the growth rate of TGS crystals was the slowest in the neutral solution (pH=2.25). It grew faster both in acidic solution (pH=1.73–2.25) and alkaline solution

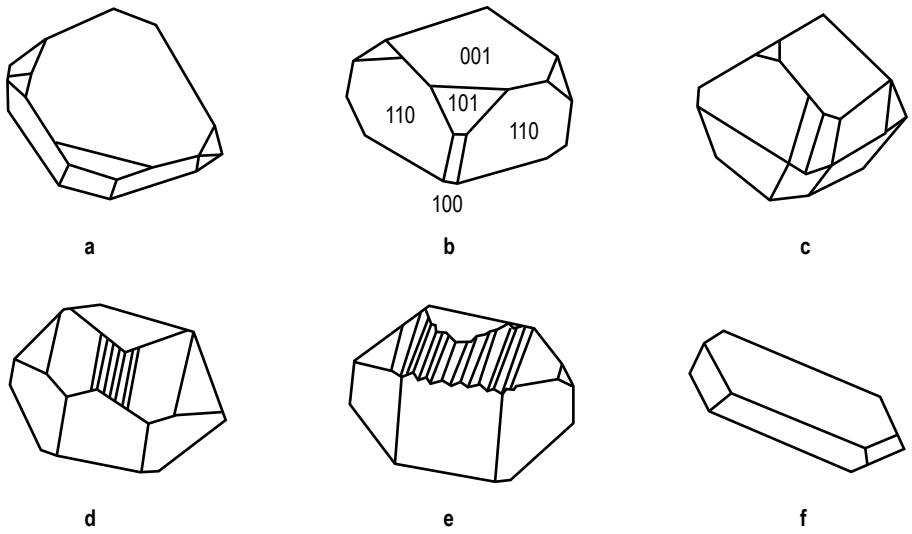

Figure 17. Change of TGS crystals habit with pH of the solution (a) 2.75, (b) 2.1, (c) 1.55, (d) 1.23, (e) 1, and (f) 0.3 (DGS).

(pH=2.25–2.52). In alkaline solution, the growth rate of TGS varied faster with the change of pH value. However, if the pH was too high, then the (010) face capped quickly. The variation of growth rate of L-alanine doped triglycine sulfophosphate (ATGSP) with pH was not similar to that of TGS. The growth rate of ATGSP crystals in a neutral solution (pH=2.5) was the fastest, and it was slower both in acidic (pH=2.2–2.5) and alkaline (pH=2.5–2.85) solutions. The above results demonstrate that on the basis of the pH of a solution, one can grow crystals at higher growth rates.

6.2.4 Effect of Impurities on Triglycine Sulfate Crystal Growth

The presence of impurities in the process of crystal growth results in modification of the crystal shape and growth rates. Different workers have studied the effects on the growth kinetics of doping TGS crystals with inorganic and organic impurities. It was observed that Ni-doped crystals were very similarin habit to pure TGS crystals, while in the case of Cu- and Fe-doped crystals the numbers of developed faces were strongly reduced.[70] In the presence of Ni, Co, and Cu ions, the rate of crystallization decreased.[80] An odd behavior was found while growing Cr-doped crystals. The addition of Cr with a concentration of 1 percent changed the regime of crystallization owing to the high chemical activity of these ions. At a concentration of about 3 percent, the rate of crystallization became very fast, even without lowering the temperature.[80] In Pd-doped crystals, the ratios of the growth rate along the *c*-axis to the growth rate along the *a* and *b* axes slightly decreased as the crystal grew larger.[85] For medium size crystals (≈30 g), the average relative growth rate along the *c*-axis was larger by more than an order of magnitude in Pd-doped crystals than in pure TGS. Pd-doped crystals also developed other faces that had not been observed before. Banan, et a1. studied the effect of Ce, Cs, L-alanine and L-alanine + Cs on the growth and morphology of TGS crystals.[81] Table 4 shows the crystal growth data and figure 18 shows their habit. The well developed (010)/(0$\bar{1}$0) faces, which were generally not present or less developed in pure TGS crystals, are obtained with L-alanine or Cs-doped crystals. Moreover, (101) faces obtained in crystals doped

Table 4. Growth data of doped TGS crystals.

Crystals	Crystal Yield g °C^{-1}/Day	Axial Growth Velocity		
		$V_{(010)}$ mm °C^{-1}/Day	$V_{(001)}$ mm °C^{-1}/Day	$V_{(010)}/V_{(001)}$
TGS	0.171	0.88	0.34	2.58
TGS + Ce	0.021	0.079	0.047	1.68
TGS + Cs	0.009	0.198	0.007	28.20
TGS + L-alanine	0.192	0.89	0.44	2.02
TGS + L-alanine + Cs	0.132	0.65	0.063	10.30

with L-alanine and in crystals doped with Cs and L-alanine were more dominant than pure TGS crystals. Also, the axial velocities, $V_{(001)}$ and $V_{(100)}$, were affected by doping (table 4). Lower growth rates were especially obvious in Cs doped crystals. The crystals became platelike for $V_{(010)}/V_{(001)} \approx 28$; and the habits were strongly disturbed (fig. 18). L-alanine doped crystals developed a habit that was asymmetric about (010) plane. The growth rate in the positive *b* direction was higher than in the negative *b* direction.[29] In D- and L-alanine doped TGS crystals, (101) faces developed more prominently than (001) faces, so the DLATGS crystals seemed to be thinner than pure TGS crystals. The (010) faces were more developed in aniline doped crystals.[84] Recently, Seif, et al. studied the dependence of growth rate of the faces of TGS and KDP crystals on concentration of Cr(III).[92] They proposed the following hypothesis to explain the effect of impurities on TGS and KDP crystals. It has long been known that when a solute crystallizes from its supersaturated solution, the presence of impurities can often have a spectacular effect on the crystal growth kinetics and the habit of the crystalline phase. The impurities exhibit a marked specificity in their action, as they are absorbed onto growing crystal surfaces. Absorption of impurities onto crystal faces changes the relative surface-free energies of the face and may block sites essential to the incorporation of new solute molecules into the crystal lattice, and hence, slow down the growth. The habit is thus, determined by slow-growing faces. Furthermore, in the TGS:Cr(III) system, doping with metal ions, metal-glycine complexes are formed in the solution and enter the crystal lattice in the growth process. The structure and type of metal-ion complexes, formed in the TGS lattice, will determine the growth rate and hence the crystal habit.

It is also worthwhile to describe the effect of the same impurity on different types of crystals. The growth kinetic data of TGS and KDP crystals grown in the presence of Cr(III) ions are presented in figures 19 and 20. This data show the effects of impurity concentration on the growth rate of different faces of TGS and KDP crystals, grown under constant low supersaturation. In the case of the KDP crystal, the mean growth rate along the [001] direction increases, while along the [100] direction it remains almost constant with a Cr(III) concentration increase in the solution/crystal and a slight fall below 7,000 ppm. A similar type of behavior/effect of Fe(III) on growth rate has been reported by Owxzarek and Sangwal.[25] $Cr_2(SO_4)_3$ molecules are considered to dissolve as an active complex such as $[Cr(H_2O)_2(OH)]^{2+}$, $[Cr(H_2O))_4(OH)_2]^{+}$, or $[Cr_2(SO_4)_2(H_2O)_7(OH)]^{+}$ and are assumed to adsorb on the crystal faces, thereby suppressing the growth rate. The impurities adsorbed on the surface of growing crystal at low supersaturation impede movements of steps by different mechanisms, depending on the site of adsorption. Models of different types that describe the adsorption process and growth reduction have been reported in the literature.[26–27,36,93] These models assume that the impurity species (ions,

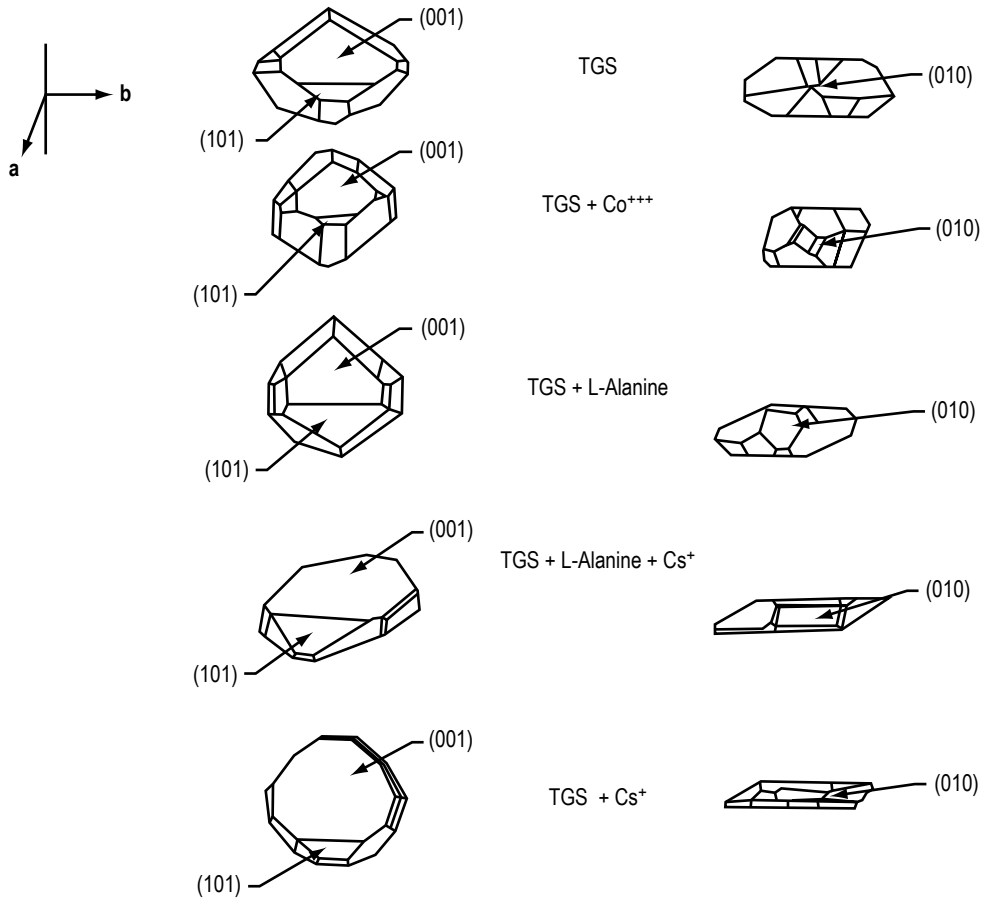

Figure 18. Growth habit of doped TGS crystals.

molecules, or atoms) are adsorbed on the crystal surface into Ks, Ls, and Ts of growing surfaces. As soon as Ks and steps are occupied by impurity particles there is a reduction in growth rate, due to coverage of the crystal faces. This decrease in the growth rate can be explained on the basis of a model proposed by Sangwal, et al. that is based on their recent studies involving the Cu(II) ammonium oxalate monohydrate crystal system.[32] As shown in figure19, the decrease in growth rate of {100} face KDP crystals should be a kinetic effect involving a reduction in the value of the kinetic coefficient ($\beta = a\nu exp^{(-W/kT)}$, where a is the dimension of growth units perpendicular to the step, ν is the frequency of vibration of molecules/atoms on the surface (s^{-1}), W is the activation energy for growth, k is the Boltzman constant, and T is the temperature (in Kelvin)) for motion of steps on the surface. Above a certain critical impurity concentration, there is no kinetic effect of impurity on growth kinetics. This may be due to the fact that all the active centers for crystallization are blocked, thus reducing the growth rate to zero. In our study, no growth of the {100} face was observed with more than 8,000 ppm of Cr(III) impurity in the KDP solution. An increase in growth rate along the [001] direction of KDP crystals may be caused by a decrease in the free energy of the face (thermodynamic effect); the surface energy decreases with an increase in impurity concentration as suggested by others, and hence, an increase in the growth rate. This discussion suggests that the kinetic or thermodynamic effect depends on the structure of the crystal face i.e atomic arrangement also besides other factors.

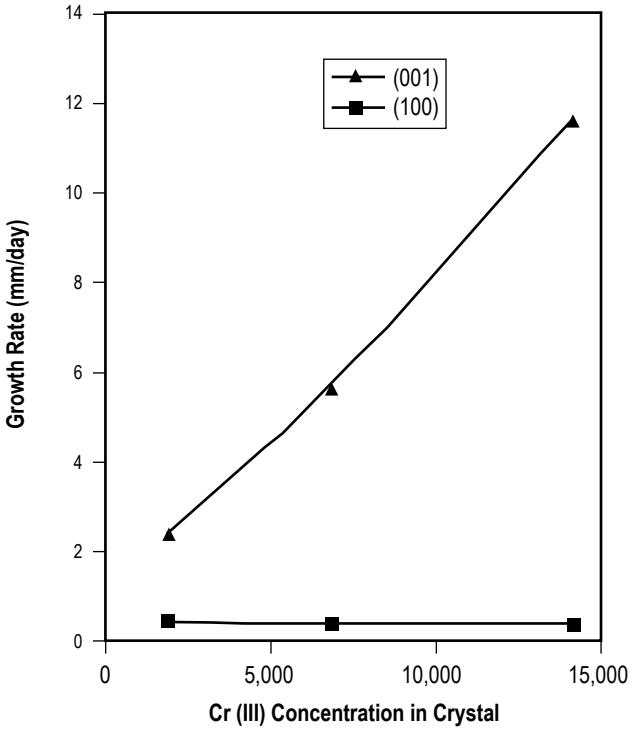

Figure 19. Growth rate dependence of the faces of KDP crystals on Cr(III) concentration.

Figure 20 shows that in the case of TGS crystals, the growth rate along the [010] direction decreases with an increase in Cr(III) concentration in the growth solution. This growth rate decrease is due to the kinetic effect, as previously explained, for the KDP crystal system. However, there is a slight increase in the growth rate along the [001] direction, with maxima around 1,300 ppm of Cr(III) and then there is a decrease. According to layer growth models, the consequence of a decrease in the edge free energy is an increase in the growth rate. Additionally, a decrease in edge free energy may cause the growth mechanism to change. The effect of an initial increase, followed by a subsequent decrease in growth rate with an increasing impurity concentration, has been suggested by Davey, et al., to opposite effects of thermodynamic and kinetic parameters.[94] Furthermore, the ability of additives to form complexes with adventitious impurities present in a growth medium cannot be ruled out, as it can alter the atomic arrangement in crystal faces. To explain the effect of impurities on growth in more detail, one needs to collect more experimental data, including studies of the micromorphology of crystal surfaces as well as growth kinetics.

Effects of various organic dopants such as L-asparagine, L-tyrosine, L-cystine, guanidine, L-valine, and others on morphology, growth, mechanical, and some physical TGS properties have also been reported in the recent past.[95–99] However, no explanation is given for the morphology change of crystals by the authors of these publications.

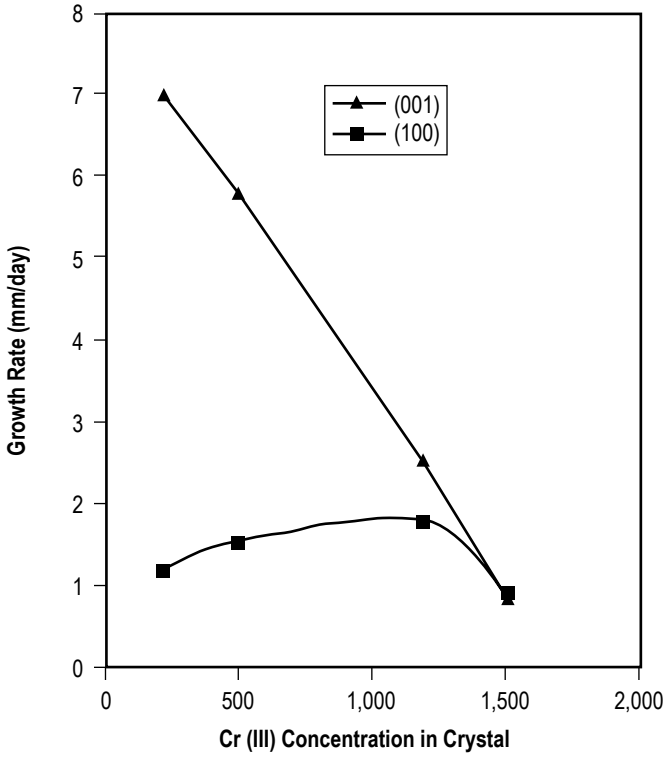

Figure 20. Growth rate dependence of the faces of TGS crystals on Cr(III) concentration.

7. SOLUTION GROWTH OF TRIGLYCINE SULFATE CRYSTALS IN MICROGRAVITY ABOARD SPACELAB–3 AND THE INTERNATIONAL MICROGRAVITY LABORATORY–1

NASA has accomplished about 115 Space Transportation Systems (STS) spaceflight missions (STS–1 to STS–121) from 1980 to present.[100]

The authors were associated with NASA's two missions called Spacelab-3 and the International Microgravity Laboratory (IML)–1 in which single TGS crystals were grown from solution in microgravity for a period of 7 days aboard the Space Shuttle.

The general goal of the programs within NASA's microgravity research division was to conduct basic and applied research under microgravity conditions (10^{-6} g) that would increase our understanding of fundamental physical, chemical, and biological processes, specifically, biotechnology, combustion science, fluid physics, fundamental physics, and materials science.

The microgravity environment of space provides a unique opportunity to further our understanding of various materials phenomena involving the molten, fluidic, and gaseous states by reducing or eliminating buoyancy-driven effects. Microgravity experiments in space are affected by residual microaccelerations on the spacecraft deriving from atmospheric drag, reaction control systems, momentum wheels, gravity gradients, crew involvement, and other disturbances. Mostly, there is no actual suggestion by the scientific community as to the microgravity level required for their experiment. The general opinion is that microgravity will reduce the influence of convection, buoyancy, and sedimentation. Hardly any quantitative estimates have been made.

The anticipated results of microgravity materials science research range from establishing baselines for fundamental materials processes to generating results with more direct commercial significance. NASA's objectives for the microgravity materials science program include:

- Advance our knowledge base for all classes of materials.
- Design and facilitate the execution of microgravity experiments that will help achieve this goal.
- Determine road maps for future microgravity studies.
- Contribute to NASA's Human Exploration and Development of Space enterprise.
- Develop enabling technologies valuable to the U.S. private sector that contributes to the National economy.

To accomplish these goals, the Materials Science program has tried to expand both its scientific scope and research community's involvement in microgravity research. Based on their requirements for

experimental facilities, most of the current materials science microgravity experiments can be divided into four general categories as follows:

- Melt growth experiments, such as those used for processing multicomponent alloys from the liquid. These experiments frequently require high temperatures and closed containers or crucibles to prevent elemental losses.

- Aqueous or solution growth experiments for materials like TGS and zeolite. These experiments usually require moderate to low temperatures. Hydrothermal processing of inorganic compounds and sol gel processing also fit in this category.

- Vapor or gaseous environments such as those used for growing mercury iodide or plasma processing.

- Processes and experiments that require containerless processing environments (unlike the other categories that use containers for the parent materials and products). Examples of these experiments include the formation of metallic and nonmetallic glasses during levitation melting and solidification, the float-zone growth of crystals, and the measurement of thermophysical properties like diffusion coefficients and surface tension.

7.1 Rationale for Solution Crystal Growth in Space

In the microgravity environment of space, several physical phenomena taken for granted on Earth change dramatically. Convection in solution due to density differences is greatly reduced. Crystallization and solidification are two processes that can benefit from the microgravity environment. As a part of NASA's Microgravity and Applications Program, a study of TGS crystal growth from solution was carried out on Spacelab-3 (SL–3) and the First International Microgravity Laboratory (IML–1) missions in 1985 and 1992 respectively. Crystals from solution are usually grown in a closed container of limited volume; thus, any convection generated tends to lead to a circular to steady laminar convection due to buoyancy. The density differences in the fluid can give rise from both temperature and concentration variations. On Earth, buoyancy-driven convection may cause microscopic gas/ solution inclusions, fluctuating dopant incorporation, and other defects in the crystals. Besides degrading pyroelectric device performance, the growth yield of useful crystals is also severely impacted due to the incorporation of these types of defects. In a low-gravity environment, convection is greatly suppressed and diffusion becomes the predominant mechanism for thermal and mass transport. Thus, growth in microgravity can eliminate these problems and enhance our knowledge about the science of crystal growth.

7.2 Solution Crystal Growth Method in Space

Since the ground solution technique could not be used in the microgravity environment of space, the authors developed a new method known as the cooled-sting technique to grow crystals in space from solution.

7.2.1 Cooled-Sting Technique

As the conventional techniques of solution crystal growth cannot be used for growing crystals in space, a new technique was proposed and developed.[100–102] On Earth, in the absence of stirring, conventional techniques of solution crystal growth cause a lowering of solution concentration in the vicinity of the growing crystal, resulting in an upward flow of solution. At constant temperature this reduction in concentration would cause the growth rate to decrease rapidly. In a 1-g environment, most solution growth techniques are directed toward increased convection mass transport by applying forced convection with very slow programmed cooling of the saturated solution. However, in the absence of convection, a change of temperature must move inward toward the crystal by conduction. The characteristic time for this to occur is $T = L^2 \rho Cp/k$, where L is the distance over which the heat must be conducted, ρ is the density, Cp is the heat capacity, and k is the thermal conductivity of solution. For water, it takes 48 min for a temperature change of 1 °C to be felt at a distance of 2 cm. This is too slow to keep a constant growth rate. So, the authors developed a unique technique that uses a programmed cooling of the seed crystal itself. This is accomplished by using a cold finger (sting) in direct contact with the seed crystal, which allows temperature lowering in accordance with a predetermined polynomial for maintaining a supersaturated TGS solution near the surface of the crystal.[103,104] Because of the L^2-dependence of T, it takes less time for a change of sting temperature to be transmitted through the growing crystal and to be felt at the surface. Construction of the ground-based cooled sting and solution growth apparatus are illustrated in figures 21 and 22 respectively.[103–105] In this case, crystals are grown by lowering the sting/seed and solution temperature, thereby creating a desired supersaturation.

7.2.2 Flight Hardware

The experiment in space utilizes the fluid experiments system (FES) and crystals are grown by a new technique developed by the authors called the cooled-sting technique as previously described.[101–103] This technique utilizes heat extraction from seed crystal through a copper rod (sting), thereby creating the desired supersaturation near the growing crystal. The sting temperature profile follows a predetermined polynomial to achieve uniform growth. Figure 23 provides a detailed diagram of the flight cell with the sting incorporated in the experimental module.[106] The FES is an apparatus with the crystal growth cell as an integral part. It was developed by NASA and fabricated by TRW, CA.

The cell is designed to allow a variety of holographic diagnostics and real-time schlieren viewing of the crystal and the surrounding fluid. Schlieren images are transmitted downlink as black and white video to reveal flow patterns and variations in fluid density. Holograms recorded in space give three-dimensional information that leads to the quantitative determination of concentration fields surrounding the crystal and the particle motion, if present, to determine g-jitters. The modified FES incorporates holographic tomography that enables taking optical data through the cell at multiple angles. During the SL–3 mission, two TGS crystals (named FES–2 and FES–3) were grown using an (001) oriented seed-type disc, as shown in figure 24. Experiment objectives of the IML–1 flight were as follows:

- Grow TGS crystals.

- Perform holographic tomography of fluid field in the test cell in three dimensions.

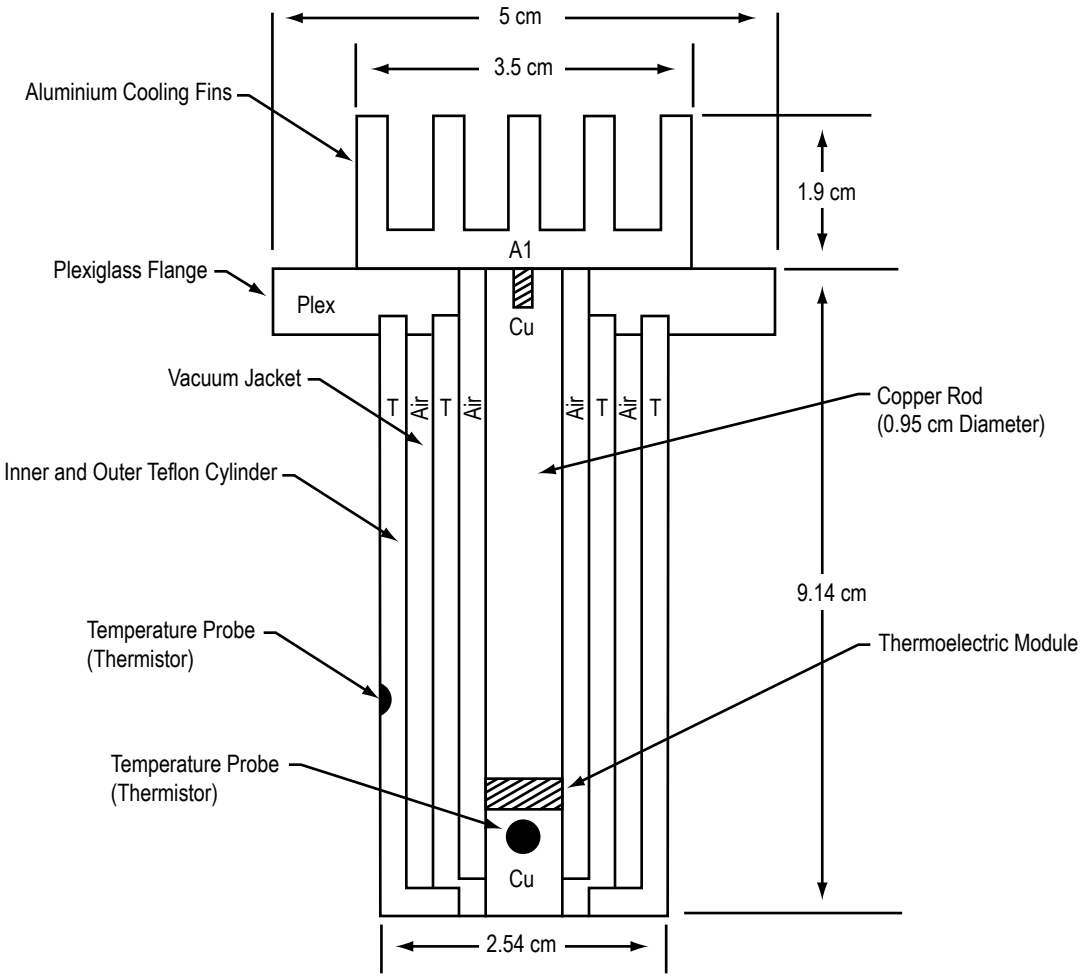

Figure 21. Laboratory version of the cooled-sting assembly for the proposed microgravity crystal growth technique.

- Study the fluid motion due to g-jitter by multiple exposure holography of tracer particles (200, 400, and 600 mm).

- Study the influence of g-jitter on crystal quality and growth rate.

R. B. Lal, one of the authors, was the Principal Investigator of the SL–3 and IML–1 experiments. The Co-Investigators were A. K. Batra, J. Trolinger, and W. R. Wilcox. Due to serious hardware problems during the IML–1 flight, only one TGS crystal was grown on an (010) oriented seed crystal. The seed crystal growth surface was a natural (010) face (unlike SL–3 experiments in which processed seeds were used) cut from a polyhedral TGS crystal, with a thickness of about 3.5 mm. TGS crystal growth rate is fast (maximum) in the [010] direction. On ground, good-quality crystals are grown on (001) oriented seed because the growth on the (010) face is nonuniform and multifaceted. Thus, it was important to investigate the growth on an (010) oriented seed in the absence of buoyancy-driven convection, where

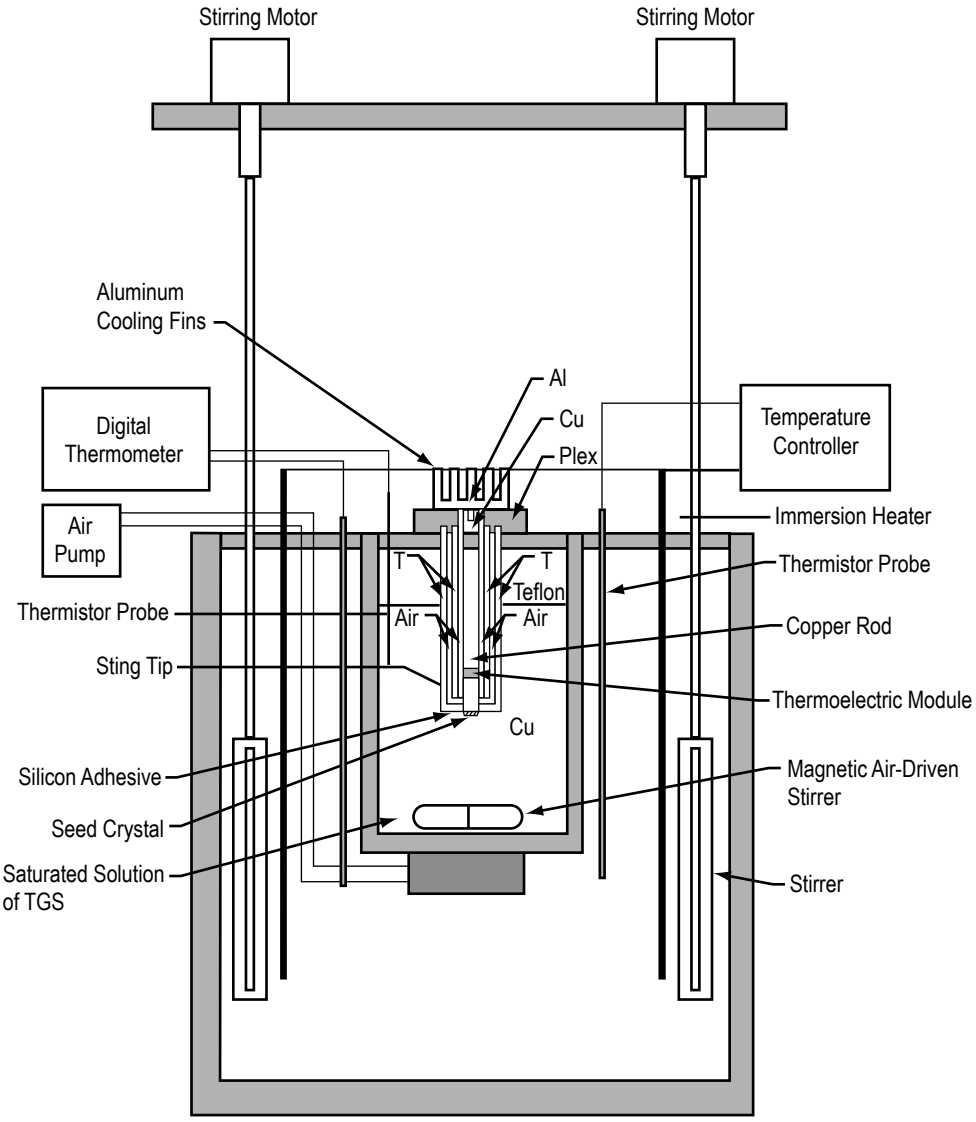

Figure 22. Schematic diagram of the ground-based cooled-sting solution growth apparatus.[102]

growth is expected to be mainly diffusion controlled. This crystal was grown with the undercooling of 4 °C for about 4 hr. The growth rate was estimated to be about 1.6 mm/day and quality of the grown crystal was substantially good. It can be attributed to a smooth transition from dissolution to growth in the space experiment.

7.2.3 Flight Optical System

The FES is a fully instrumented spaceflight chamber that can characterize the growth process through diagnostics of the crystal environment. The layout of the optical system is shown in figure 25. Optical diagnostic instruments include two holographic cameras and a schlieren system, the output of which can be viewed in real time by TV downlink. The optical and electronic instruments provide the measure of solution concentration, temperature, convection, growth rate, and crystal properties during the time of growth.

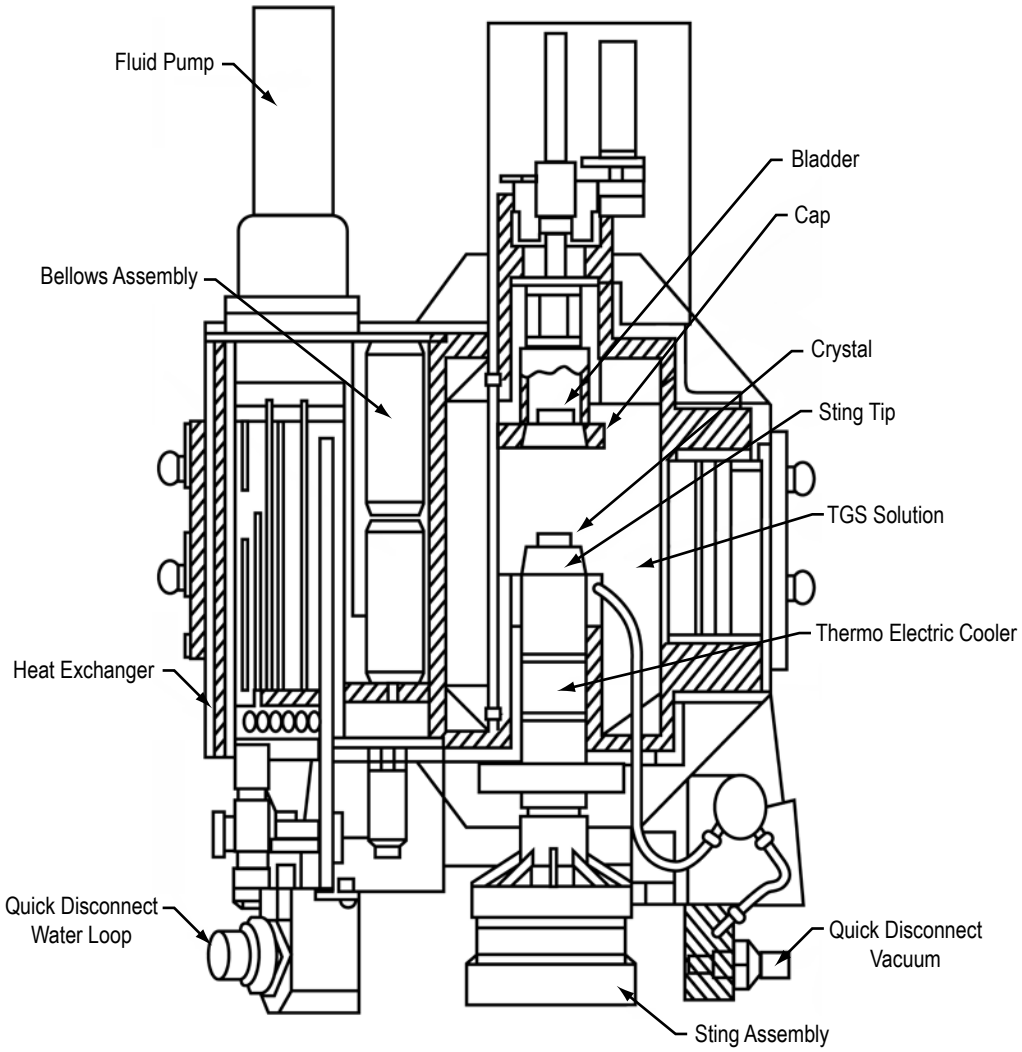

Figure 23. Flight crystal growth cell designed and developed by NASA.

By recording light passing through the cell, as well as light scattered from the crystal, holography provides diagnostics of the fluid through holographic interferometry, and particle diagnostics through three-dimensional particle imaging velocimetry. Figure 26 shows the optical system layout in which a 4-in diameter collimated He Ne (Spectra Physics 107) laser beam passes through a double window into the crystal growth chamber, through the TGS solution, across the surface of the crystal, and finally emerging from a second set of windows. The beam then continues to the hologram plane, approximately 20-cm away, where it is mixed with a collimated reference wave on 70-mm format roll film. The film is drawn flat on the platen by a vacuum in a unique film implementation of hologram recording for interferometry. In addition to the use of vacuum platens for recording and reconstruction, a special reconstruction process, necessary for holographic interferometry with film, was developed to account for the imperfect optical quality of the film. A second holocamera views the crystal face directly from a lateral window.[107] Four types of holograms were produced including single- and multiple-exposed holograms. Back lighting of the crystal was accomplished in two different ways, each with advantages and limitations: 1) Direct laser beam and 2) diffuse beam. Direct illumination is used for interferometry and schlieren. With

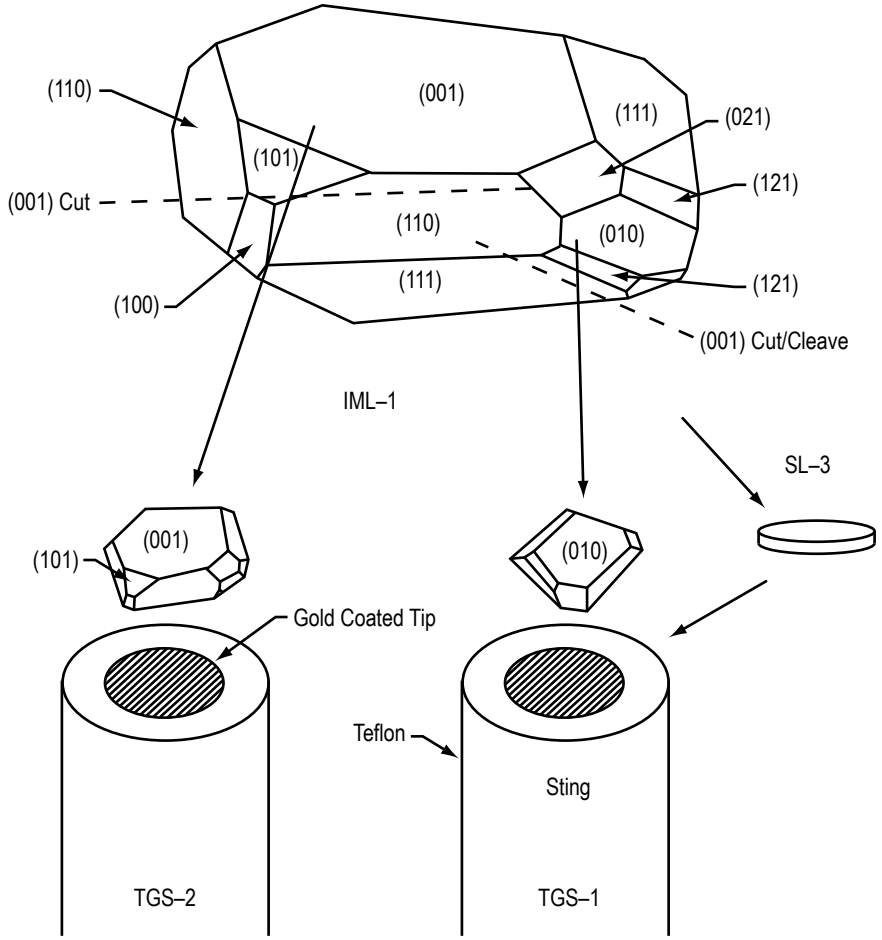

Figure 24. TGS seed crystals used for growth runs on the IML–1 mission.

conventional optics, the direct illumination beam would provide a single illumination and viewing angle through the field. The diffuse beam is produced by inserting a diffuser into the object beam path before the beam enters the first cell window. The diffuse beam illuminates the field with many directions and is convenient for some types of viewing; however, such illumination is not useful for interferometry or schlieren in this system.

Previous SL–3 experience taught us that more than one viewing angle is desirable. Multiple viewing angles were achieved in IML–1 through the use of windows equipped with holographic optical elements (HOEs). The input window contains HOEs that convert the single-input beam into three beams that pass over the crystal at angles of 0° and ± 23.5°. The opposite window contains HOEs that redirect these beams to the recording film plane so they can all be recorded and again separated during reconstruction. Consequently, each recording comprises three superimposed but independently viewable holograms. The schlieren system is viewed by T' that allows real-time viewing by both the crew and the TV downlink. A primary use of the schlieren system is to view and judge the transition of the crystal from a dissolution phase to a growth phase, since control of this transition is considered to be critical in producing a high-quality crystal. In the schlieren system, the knife-edge was set so that as the crystal was dissolving, light rays entering the resulting higher refractive index region above the crystal would be refracted in the

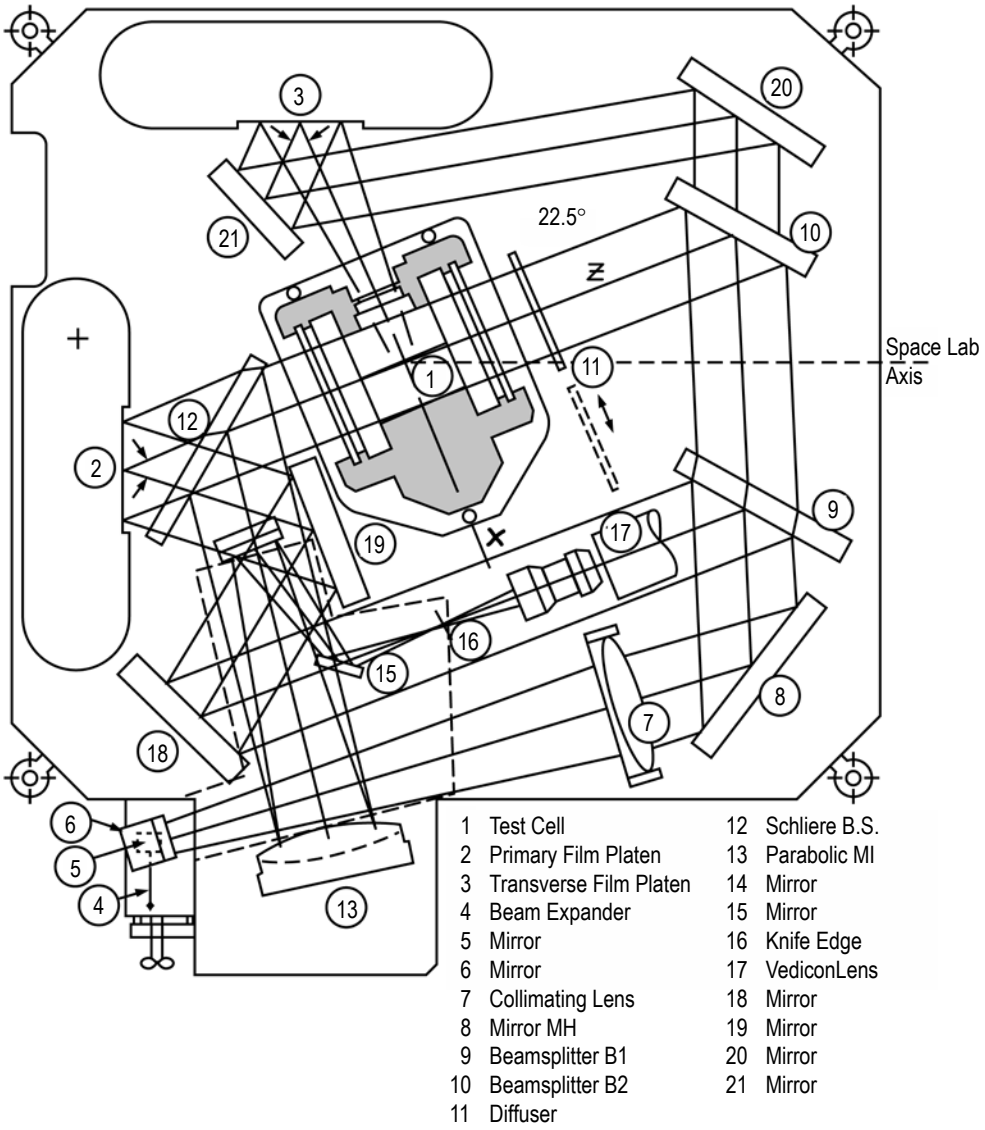

Figure 25. Modified FES optical system with various components.

direction of the crystal to be removed by the knife-edge, these appear dark in the image. After the transition from dissolving to growing was made, the region immediately above the crystal would be depleted of solute, thus reducing the refractive index and causing the refracted rays to pass above the knife edge, causing a bright region to appear above the crystal within the larger dark region of higher concentration. This method proved to be an extremely sensitive way to identify the transition from dissolving to growth.

7.3 Results and Discussion

The flight TGS crystals were examined with a high-resolution monochromatic synchrotron x-radiation diffraction technique, both before and after slicing for the fabrication of infrared detectors to check the lattice regularity, identify inclusions and dislocations, draw inferences about growth mode

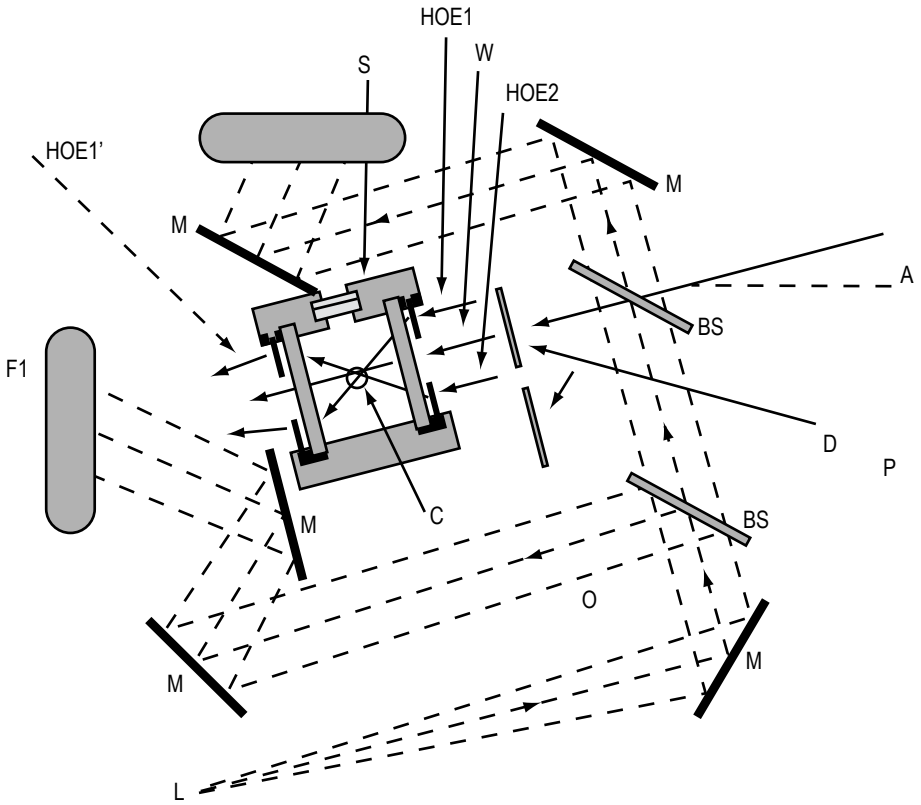

Figure 26. Detailed optical layout of the FES, designed and developed by TRW, consisting of the following components: A—angle between the optical axis and the Space Shuttle axis, M—mirror, BS—beamsplitter, C—crystal, O—lens, D—removable diffusor, F1—hologram 1, F2—hologram 2, L—HeNe laser underneath, and S—side window. Note that the ray emerges at an angle to simplify separation.

and stability, and locate the interface between the seed and the new growth. The experiments were performed at the National Synchrotron Light Source at Brookhaven National Laboratory in collaboration with Dr. Bruce Steiner of the National Institute of Standards and Technology (NIST). The performance of the materials was determined by their structure, and in this performance irregularity typically played a leading role. The growth of crystals in low-g has long been of interest because of the anticipation that a reduction in gravitational forces would strongly affect crystal growth, and therefore, the nature of resulting irregularities. Many factors affect crystal growth, and because these can interact strongly with one another, the understanding of the structural variation necessary for effective exploitation has not been fully achieved. A knowledge of irregularities in space-grown and Earth-grown crystals, developed in conjunction with an understanding their genesis and detailed effects on properties, would be an important challenge. Such knowledge is also expected to dramatically improve single-crystal production, both in space and on Earth. The local acceptance angle for diffraction from the uncut flight TGS–1 crystal, 1–2 arc sec (fig. 27), indicates extraordinary crystal quality.[108] Polystyrene particles that had been included in the space-grown material in the IML–1 experiment are observed as small imperfections, as shown in figure 27 (b). Also, the faceted growth mode is clearly distinguishable in figure 27 (b). Two sets of edge dislocations in the seed, the [101] oriented and the [001] oriented, were noted as well in images taken in Laue geometry, but they appear not to have affected the space growth. Observation

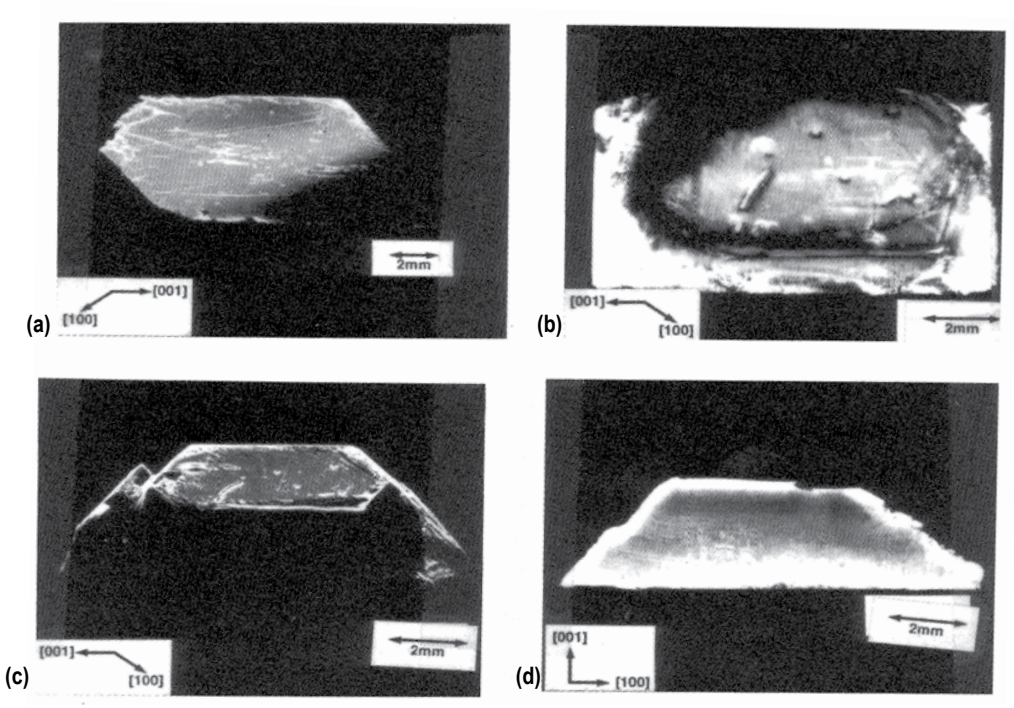

Figure 27. High-resolution synchrotron x-ray radiation diffraction imaging of 1-g and μg grown TGS crystals.

of the cut edge of the crystal, figure 27 (d), shows continuity between the seed at the top. Demarcation between the seed and the space-grown material is indistinct. High-resolution imaging of terrestrial crystals has shown that the surface treatment of the seed crystal is critical to growth perfection. Ground-control TGS crystals were of extremely high perfection. A slice next to many possible flight seeds was examined by high-resolution diffraction imaging. Flight seed selection was based on the perfection of the slice next to the seed crystal.

Infrared detectors from the flight- and ground-control crystals were fabricated at EDO/Barnes Engineering Division, Shelton, CT. The detectivity (D^*) and other parameters for these infrared detectors are shown in figure 28 and the detector characteristics are given in table 5. The detectivity (D^*) for IR detectors fabricated from the IML–1 crystal shows an improvement over the ground-grown crystals and crystals grown on SL–3.

Particle motion of three different sized particles were mapped using the techniques described previously.[106,107] The combined effects of fluid convection, particle interaction, residual gravity, shuttle maneuvers, and g-jitters have been observed. The interferograms, however, show several noteworthy features. When the crystal enters a growth phase, the solution in the region near the crystal is depleted of solute, thus reducing the refractive index below the surrounding fluid, creating a hemispherical cap of fringes over the crystal, as shown in figure 29. The stability of this cloud in the interferograms confirmed that the crystal was growing in a diffusion-controlled process. The cloud did show, however, that the process was not completely axisymmetric, a condition caused by equipment problems that were encountered during the mission.

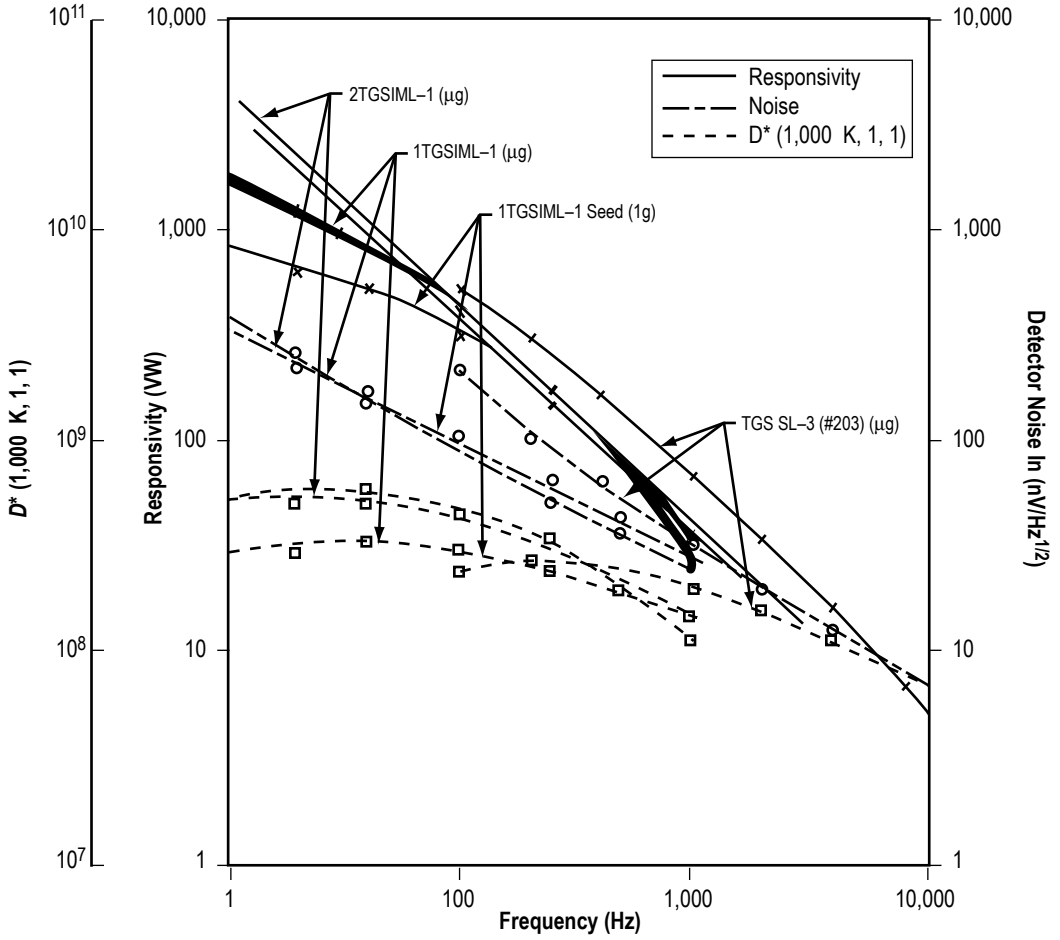

Figure 28. Relevant parameters of IR detectors fabricated from 1-g and μ-g grown TGS crystals.

Table 5. Detector characteristics of space-grown TGS crystals.

Crystal (TGS)	Noise nV/Hz$^{1/2}$	Responsivity (V/W)	Detectivity (1,000 K,f,1) $\times 10^8$	f Hz	Remarks
SL–3/FES2–TGS (μg-grown)	320	510	0.99	100	Area = 0.3×3 mm, blackened
IML–1TGS Seed (1g-grown)	418	320	2	100	Area = 1×1 mm, no window
IML–1TGS (μg-grown)	90	400	4.2	100	Area = 1×1 mm
IML–1TGS (1g-grown)	98	420	4.5	100	Area = 1×1 mm
IML–1TGS (μg-grown)	100	340	3	100	Area = 1×1 mm

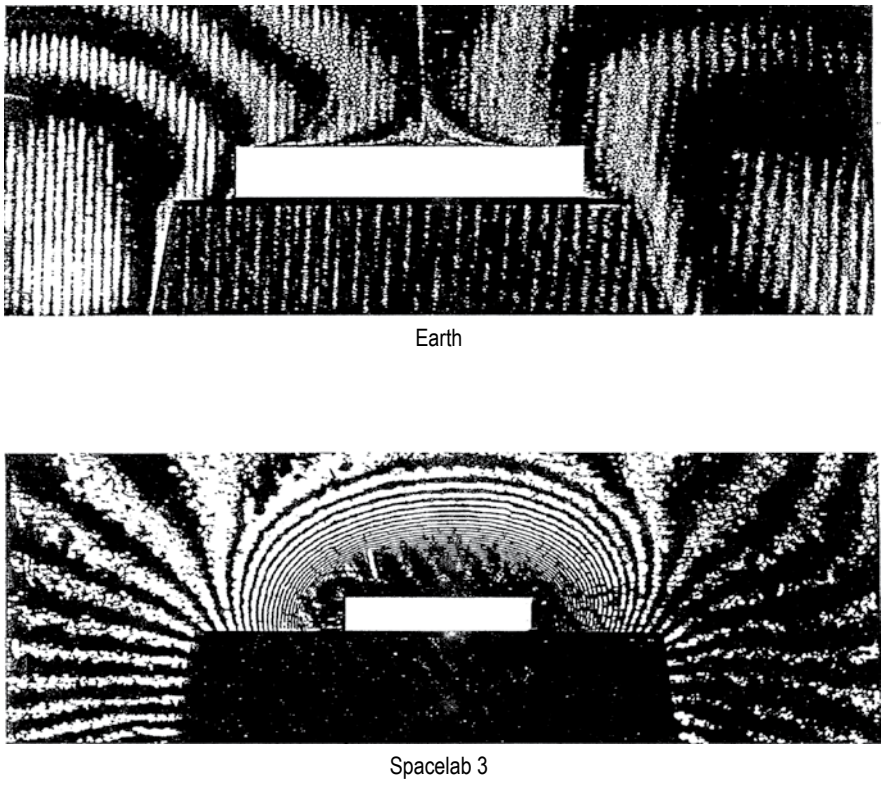

Figure 29. Interferograms of concentration field in TGS solution on Earth and in microgravity onboard SL–3.

To summarize, two important objectives were attained in the IML–1 experiment, in spite of FES operation problems: 1) A high-quality TGS crystal was grown and 2) the particle dynamics experiment was successful.

In spite of limited time and fast growth, the growth on the (010) face was substantially uniform over a period of 18 hr. The growth on the (010) face on ground is mostly nonuniform. The local acceptance angle for diffraction from the uncut crystal, 1–2 arc sec, indicates extraordinary crystal regularity.

Three sizes of polystyrene particles that had been occluded by the growing TGS were observed as small imperfections in the grown crystal. Observations of the cut edge of the flight crystal (TGS–1) show continuity between the seed at the bottom and the space growth at the top, indicating a high degree of epitaxy of the space-grown material. Demarcation between the seed and the space-grown material is indistinct, indicating a smooth transition from dissolution to growth, so solvent inclusions between the seed and the grown layer are not formed. Experiments on Earth have shown that such inclusions tend to result in dislocations that propagate through subsequently grown material and degrade properties. The IR detectors fabricated from the TGS–1 flight crystal show improved detectivity (D^*) compared to ground samples and even with detectors fabricated from crystals grown on SL–3. The dielectric loss in the IML–1 crystal is lower than in ground crystals and crystals grown in SL–3.

8. PROTEIN CRYSTAL GROWTH

The human body contains thousands of different proteins that play essential roles in maintaining life. A protein's structure determines the specific role that proteins play in the human body; however, researchers lack detailed knowledge about the structures of many proteins. Crystallization of proteins has three major applications: 1) Structural biology and drug design, 2) bioseparations, and 3) controlled drug delivery. In the first application, protein crystals are used with crystallography techniques to ascertain the three-dimensional structure of the molecule. This structure is indispensable in correctly determining the complex biological functions of these macromolecules. Drug design involves designing a molecule that can fit exactly into a binding site of a macromolecule and block function of the disease pathway. Producing better quality crystals will result in a more accurate three-dimensional protein structure, which in turn, means the biological function can be known more precisely resulting in improved drug design. Bioseparations refer to the downstream processing of the fermentation products. Typically, the desired product of the fermentation process is a protein (e.g. insulin) that needs to be separated from the biomass. Crystallization is one of the commonly employed techniques for protein separation. It has the advantage of being a benign separation process that does not cause the protein to unfold and lose its activity. Controlled drug delivery is also very important. Most drugs rapidly clear the body following administration, making it difficult to achieve a constant desired level over a period of time. When the drug is a protein, such as insulin or Alfa-interferon, administrating the drug in the crystalline form shows promise of achieving controlled delivery. The challenge is to produce crystals of relatively uniform size so that dosage can be prescribed correctly.

8.1 Protein Crystal Growth Methods

Protein crystallization is inherently difficult because of the fragile nature of protein crystals. Proteins have irregularly shaped surfaces that result in the formation of large channels within any protein crystal. Therefore, the no-covalent bonds that hold the lattice together must often be formed through several layers of solvent molecules. In addition to overcoming the inherent fragility of protein crystals, successful production of x-ray worthy crystals is dependent upon a number of environmental factors because so much variation exists among proteins, with each individual requiring unique conditions for successful crystallization. Therefore, attempting to crystallize a protein without a proven protocol can be very tedious. Factors that require consideration are protein purity, pH, protein concentration, temperature, and precipitants. To initiate crystallization, the protein solution has to be brought to a thermodynamically unstable state of supersaturation. The solution can be brought back to the stable equilibrium state through precipitation of the protein, which is the most frequent process, or through crystallization. The supersaturation state can be achieved by several techniques including evaporation of solvent molecules, change of ionic strength, change of pH, change of temperature, or change of some other parameter.

Two of the most commonly used methods for protein crystallization are: 1) Hanging drop method and 2) sitting drop method, which falls under the category of vapor diffusion[109–110] Both of these methods entail a droplet containing purified protein, buffer, and precipitants in higher concentration. Initially, the droplet of protein solution contains an insufficient concentration of precipitant for crystallization, but as water vaporizes from the drop and transfers to the reservoir, the precipitant concentration increases

to a level optimal for crystallization. Since the system is in equilibrium, these optimum conditions are maintained until crystallization is complete. Figures 30 and 31 depict the hanging drop and sitting drop systems, respectively. The hanging drop method differs from the sitting drop method in the vertical orientation of the protein solution drop within the system. It is important to mention that both methods require a closed system, meaning the system must be sealed off from the outside using an airtight container. It is also worthy of mentioning that the reservoir solution usually contains buffer and precipitant. The protein solution contains the same compounds, but in lower concentrations. For precipitation, the protein solution may also contain trace metals or ions. For instance, insulin is known to require trace amounts of zinc for crystallization.

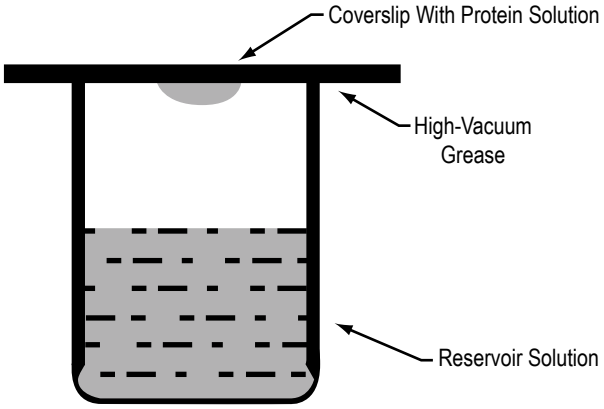

Figure 30. Schematic diagram of the hanging drop method.

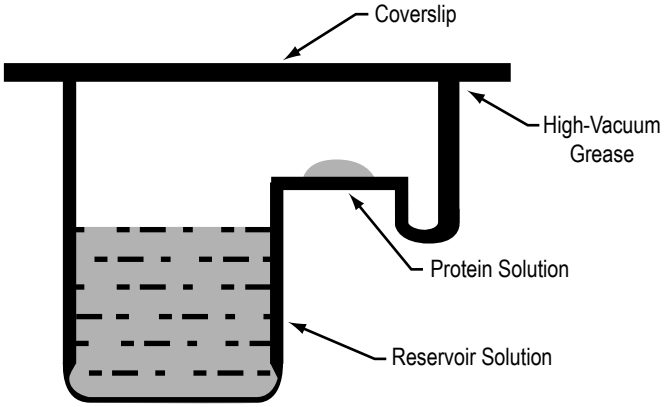

Figure 31. Schematic diagram of the sitting drop method.

8.2 Protein Crystal Growth Mechanisms

From the presence of well-defined facets on most protein crystals, one can unambiguously conclude that growth occurs via the spreading of layers from growth step sources such as dislocations and two-dimensional nuclei. This has been confirmed on a molecular level. Ex situ electron microscopy

observations have resolved individual growth steps on (010) and (110) faces of tetragonal lysozyme that, contrary to recent claims are of monomolecular height.[111–113] In situ atomic force microscopy of lysozyme has produced particularly instructive images of growth step generation at screw dislocation outcrops and of two-dimensional nucleation-induced islands.

Most recently, atomic force microscopy observations on a larger number of other proteins and viruses have reproduced the whole body of growth morphology and kinetic scenarios known for inorganic solution growth including the following: [114]

- Layer spreading from dislocations.
- Two-dimensional nuclei interaction between growth steps from sources of different activities.
- Impediment of step propagation by foreign particles.

Particle engulfment was often observed to result in dislocation formation. Crystallites that impinged on the interface became either epitaxially aligned with the main crystal or remained misaligned and caused various defects during further growth. There even appears to be some indication of kinetic roughening on certain facets of some proteins.[115]

8.3 Protein Crystal Growth in Microgravity

The microgravity environment aboard spacecraft in low-Earth orbit provides a convection and sedimentation free environment for the study and application of fluid-based systems.[116–117] With the advent of the Space Shuttle, scientists had regular access to such environments and many experiments were initiated, including those in protein crystallization. After many trials, it became clear that for several proteins, crystallization in microgravity environment resulted in bigger and better crystals. In some instances, crystals that could not be crystallized at all on the ground were found to crystallize in space. Conversely, for numerous proteins the space environment was found to be no better or was even worse than ground-based conditions. As a result of these observations, NASA has become one of the leading Federal agencies in prompting and funding protein crystallization research. Efforts are directed at both utilizing the space environment to improve crystallization of novel proteins and in fundamental studies of the causes (if any) of the improvement in protein crystals produced in microgravity. The results from flying more and studying in more detail have significantly altered attitudes toward space-based protein crystal growth. Persuasive explanations and a strong theoretical model have emerged to explain why space-based growth is better.

Since the inception of protein crystal growth in microgravity research by Littke, several research groups have developed microgravity hardware and experiments, including the following:[118–123]

- Hand-held protein crystallization apparatus for microgravity (HH–PCAM).[124]
- Diffusion-controlled crystallization apparatus for microgravity (DCAM).[125]
- High-density protein crystal growth system (HDPCG).[126]

- Protein crystallization facility (PCF).[127]
- A multiuser facility-based protein crystallization apparatus for microgravity (PCAM).[124]
- Advanced protein crystallization facility (APCF).[125]

Several thousand individual protein crystal growth experiments have been flown using the PCAM facility hardware aboard the Space Shuttle. According to the developer, this facility hardware represents a pioneering development in design and deployment of spaceflight hardware based on disposable interface elements.[124] Furthermore, it has resulted in an ultrahigh resolution structure and the first example of neutron diffraction achieved as a result of protein crystal growth in microgravity.[127] Additionally, fundamental differences in protein partitioning in microgravity have been documented, using this facility, that represent the first direct experimental observation of the factors contributing to quality improvements in the growth of protein crystals in microgravity.[128] The other important hardware, referred to as DCAM, utilizes the dialysis method and allows the equilibration rate of each individual experiment to be passively controlled from several days to several months. It is worth mentioning that the supersaturation precision control rate in this hardware has routinely produced macrocrystals for a variety of proteins, sized from 5 mm to 1.25 cm. Analysis of serum albumin, ferritin, lysozyme, bacteriorhodopsin, and nucleosome core hardware improvements for the International Space Station will allow scientists to learn more about the growth mechanisms and perform x-ray analysis aboard the Space Station.[126]

9. CONCLUDING REMARKS

Bulk, high-quality, single crystals are required for use in fabricating devices for various technological applications. Crystal growth is a complicated process that depends on many parameters that can interact and the complete process is not well understood. This is one of the reasons to grow crystals in the microgravity of space to separate omnipresent convection on Earth and have only diffusion-controlled growth. Authors have attempted to give a comprehensive overview of the various problems encountered in the solution growth of single crystals on Earth and in-space experiments based on their experience for almost three decades. The solutions of the various problems encountered during growth on ground and in spaceflight experiments are described. This section serves as a foundation for those who desire to initiate a research program in the growth of bulk single crystals of technological importance that can be grown from the low-temperature solution technique. A brief review of crystal growth fundamentals is presented, including key techniques for solution crystal growth such as solubility determination and the design of various crystal growth systems including the mechanical and electronic crystal motor reciprocating arrangement. Three generations of modifications to solution crystallizers designed and fabricated in the laboratory and the crystallizer for the space growth cooled-sting technique advanced by the authors are described. A number of solution-grown crystals grown at Alabama A&M University are shown. A detailed description of the crystal growth experiments on TGS, an important IR material is provided, along with an explanation of the difficulties encountered with SL–3 and IML–1 crystal growth experiments aboard the Space Shuttle. The basic principles that are shared by the solution growth technique and protein crystal growth are briefly mentioned and the efforts of protein crystal growth in microgravity are also discussed.

REFERENCES

1. Meirs, H.A.; and Isaac, F: "The Spontaneous Crystallization," *Proc. Roy. Soc. London*, Vol. A79, pp. 322–325, 1907.

2. Sangwal, K.: "Growth Kinetics and Surface Morphology of Crystals Grown From Solutions: Recent Observations and Their Interpretations," *Prog. Cryst. Growth and Charact. Mat.*, Vol. 36, No. 3, pp. 163–248, 1998.

3. Nicolau, I.F.: "Growth Kinetics of Potassium-Dihydrogen Phosphate Crystals in Solution," *Kristall and Technik*, Vol. 9, No. 11, pp. 1255–1263, 1974.

4. Janssen-Van Rosmalen, R.; Bennema, P.; and Garside, J.: "The Influence of Volume Diffusion on Crystal Growth," *J. Cryst. Growth*, Vol. 29, pp. 342–352, 1975.

5. Chianese, A.: "Growth and Dissolution of Sodium Perborate in Aqueous Solutions by Using the RDC Technique," *J. Cryst. Growth,* Vol. 91, pp. 39–49, 1988.

6. Sangwal, K.: "On the Mechanism of Crystal Growth From Solutions—An Introduction," *J. Cryst. Growth*, Vol. 192, pp. 200–214, 1998.

7. Wang, Y.; Yu, X.L.; Sun, D.L.; and Yin, S.T.: "Mass Transport and Growth Kinetics Related to the Interface Supersaturation on Lithium Formate Monohydrate," *Cryst. Res. Technol.*, Vol. 36, No. 4–5, pp. 441–448, 2001.

8. Zaitseva, N.; and Carman, L: "Rapid Growth of KDP-Type Crystals," *Prog. Cryst. Growth and Charact. Mat.*, Vol. 43, No. 1, pp. 1–118, 2001.

9. Melikhov, I.V.; and Berliner, L.B.: "Crystallization of Salts From Supersaturated Solutions, Diffusion Kinetics," *J. Cryst. Growth*, Vol. 46, No. 1, pp. 79–84, 1979.

10. Bennema, P.: "Spiral Growth and Surface Roughening: Developments Since Burton, Cabrera and Frank," *J. Cryst. Growth*, Vol. 69, pp. 182–197, 1984.

11. Liu, X.Y.: Malwa, K.; and Tsukamoto, K.: "Heterogeneous Two-Dimensional Nucleation and Growth Kinetics," *J. Chem. Phys.*, Vol. 106, No. 5, pp. 1870–1879, 1997.

12. Izmailov, A.F.; and Myerson, A.S: "Momentum and Mass Transfer in Supersaturation Solutions and Crystal Growth From Solution," *J. Cryst. Growth*, Vol. 174, pp. 362–368, 1997.

13. Rak, M.; Izdebski, M.; and Brozi, A.: "Kinetic Monte Carlo Study of Crystal Growth From Solution," *Computer Phys. Comm.*, Vol. 138, No. 3, 250–263, 2001.

14. Mutaftschiev, B.: *Interfacial Aspects of Phase Transformation,* NATO Science Series C, D. Reidel Publishing Company, Hingham, MA, 1982.

15. Chernov, A.A.: "Present Day Understanding of Crystal Growth From Aqueous Solutions," *Prog. Cryst. Growth and Charact. Mater.*, Vol. 26, No. 95, pp. 121–151, 1993.

16. Mohan, R.; and Myerson, A.S.: "Growth Kinetics: A Thermodynamic Approach," *Chem. Engn. Sci.*, Vol. 57, No. 20, pp. 4277–4285, 2002.

17. Pina, C.M.; Putnis, A.; and Astilleros, J.M.: "The Growth Mechanisms of Solid Solutions Crystallizing From Aqueous Solutions," *Chemical Geology*, Vol. 204, No. 1–2, pp. 145–161, 2004.

18. Sunagawa, I.; Tsukamoto, K.; Maiwa, K.; and Onuma, K.: "Growth and Perfection of Crystals From Aqueous Solution: Case Studies on Barium Nitrate and K-Alum," *Prog. Cryst. Growth Charact. Mater.*, Vol. 30, No. 2–3, pp. 153–190, 1995.

19. Wilcox, W.R.: "Influence of Convection on the Growth of Crystals From Solution," *J. Cryst. Growth*, Vol. 65, pp. 133–142, 1983.

20. Markov, I.V.: *Crystal Growth for Beginners: Fundamentals of Nucleation, Crystal Growth, and Epitaxy,* World Scientific, NJ, 2003.

21. Sunagawa, I.: *Crystals: Growth, Morphology, and Perfection*, Cambridge University Press, Cambridge, UK, 2005.

22. Ogawa, T.: "A Phenomenological Analysis of Crystal Growth From Solutions as an Irreversible Process," *Jap. J. Appl. Phys.*, Vol. 16, No. 5, pp. 689–695, 1977.

23. Veintemillas-Verdaguer, S.: "Chemical Aspects of the Effect of Impurities in Crystal Growth," *Prog. Cryst. Growth Charact. Mater.*, Vol. 32, pp. 76–109, 1996.

24. Sangwal, K.: "Kinetic Effects of Impurities on the Growth of Single Crystals From Solutions," *J. Cryst. Growth,* Vol. 203, No. 1, pp. 197–212, 1999.

25. Owczarek, I.; and Sangwal, K.: "Effect of Impurities on the Growth of KDP Crystals: Mechanism of Adsorption on (101) Faces," *J. Cryst. Growth*, Vol. 102, No. 3, pp. 574–580, 1990.

26. Sangwal, K.: "Effects of Impurities on the Crystal Growth Processes," *Prog. Cryst. Growth Charact. Mater.*, Vol. 32, No. 1–3, pp. 3–43, 1996.

27. Kirkova, E.; Djarova, M.; and Donkova, B.: "Inclusions of Isomorphism Impurities During Crystallization From Solutions," *Prog. Cryst. Growth Charact. Mater.*, Vol. 32, No. 1–3, pp. 111–134, 1996.

28. Rauls, M.; Bartosch, K.; Kind, M.; Kuch, S.; Lacmann, R.; and Mersmann, A.: "The Influence of Impurities on Crystallization Kinetics—A Case Study on Ammonium Sulfate," *J. Cryst. Growth Charact. Mater.*, Vol. 213, No. 1, pp. 116–128, 2000.

29. Mielniczek-Brzoska, E.; Gielzak-Kocwin, K.; and Sangwal, K.: "Effect of Cu(II) Ions on the Growth of Ammonium Oxalate Monohydrate Crystals From Aqueous Solutions: Growth Kinetics, Segregation Coefficient and Characterization of Incorporation Sites," *J. Cryst. Growth Charact. Mater.*, Vol. 212, No. 3, pp. 532–542, 2000.

30. Sangwal, K.; Mielniczek-Brzoska, E.; and Bore, J.: "Effect of Mn(II) Ions on the Growth of Ammonium Oxalate Monohydrate Crystals From Aqueous Solutions: Growth Habit and Surface Morphology," *Cryst. Res. Technol.*, Vol. 38, No. 2, pp. 103–112, 2003.

31. Kubota, N.; Yokota, M.; and Mullin, J.W.: "Supersaturation Dependence of Crystal Growth in Solutions in the Presence of Impurity," *J. Cryst. Growth*, Vol. 182, No. 1, pp. 86–94, 1997.

32. Sangwal, K.; and Mielniczek-Brzoska, E.: "On the Effect of Cu(II) Impurities on the Growth Kinetics of Ammonium Oxalate Monohydrate Crystals From Aqueous Solutions," *Cryst. Res. Technol.*, Vol. 36, No. 8–10, pp. 837–849, 2001.

33. Sangwal, K.; Mielniczek-Brzoska, E.; and Bore, J.: "Study of Segregation Coefficient of Cationic Impurities in Ammonium Oxalate Monohydrate Crystals During Growth From Aqueous Solutions," *J. Cryst. Growth*, Vol. 244, No. 2, pp. 183–193, 2002.

34. Sangwal, K.; and Palcznska, T.: "On the Supersaturation and Impurity Concentration Dependence of Segregation Coefficient in Crystals Grown From Solutions," *J. Cryst. Growth,* Vol. 212, No. 3, pp. 522–531, 2000.

35. Delineshev, S.P.: "Growth of Crystals in the Presence of Impurities, A Hypothesis Based on a Kinetic Approach," *Cryst. Res. Technol.*, Vol. 33, No. 6, pp. 891–897, 1998.

36. Sangwal, K.: "Kinetic Effects of Impurities on the Growth of Single Crystals From Solutions," *J. Cryst. Growth*, Vol. 203, No. 1–2, pp. 197–212, 1999.

37. Myerson, A.S.; and Jang, S.M.: "A Comparison of Binding Energy and Metastable Zone Width for Adipic Acid With Various Additives," *J. Cryst. Growth*, Vol. 156, No. 4, pp. 459–466, 1995.

38. Aquilano, D.; Rubbo, M.; Mantovani, G.; Sgualdino, G.; and Vaccari, G.: "Equilibrium and Growth Forms of Sucrose Crystals in the {h0l} Zone I: Theoretical treatment of {101}-d form," *J. Cryst. Growth*, Vol. 74, No. 1, pp. 10–20, 1986.

39. Aquilano, D.; Rubbo, M.; Mantovani, G.; Sgualdino, G.; and Vaccari, G.: "Equilibrium and Growth Forms of Sucrose Crystals in the {h0l}Zone," *J. Cryst. Growth*, Vol. 83, pp. 77–83, 1987.

40. Chernov, A.A.; and Sipyagin, V.V.: "Peculiarities in Crystal Growth Aqueous Solutions Connected With Their Structure," *Current Topics in Materials Science*, E. Kaldis, Ed., Vol 5, pp. 279–333, North-Holland, Amsterdam, 1980.

41. *Crystal Growth of Technologically Important Electronic Materials*, K. Byrappa, H. Klapper, T. Ohachi, and R. Fornari Eds., Allied Publishers PVT. Limited, New Delhi, 2003.

42. Aggarwal, M.D.; Gebre, T.; Batra, A.K.; et al.: "Growth of Nonlinear Optical Materials at Alabama A&M University," *Proc. of SPIE*, Vol. 4813, *Crystal Materials for Nonlinear Optical Devices and Microgravity Science*, pp. 52–65, 2002.

43. Aggarwal, M.D.; Wang, W.S.; Bhat, K.; Penn, P.G.; and Frazier, D.O.: "Photonic Crystals: Crystal Growth Processing and Physical Properties," *Handbook of Advanced Electronic and Photonic Materials and Devices*, H. S. Nalwa. Ed., Academic Press, New York, NY, Vol. 9, pp. 193–228, 2001.

44. Henisch, H.K.: *Crystal Growth in Gels,* Dover Publications, Inc., New York, NY, 1970.

45. Barton, A.F.: *Handbook of Solubility Parameters and Other Cohesion Parameters*, CRC Press, Boca Raton, FL, 1983.

46. Novotny, J.: "A Crystallizer for the Investigation of Conditions of Growth of Single Crystals From Solutions," *Kristall and Technik*, Vol. 6, No. 3, pp. 343–352, 1971.

47. Aggarwal, M.D.; Choi, J.; Wang, W.S.; et al.: "Solution Growth of a Novel Nonlinear Optical Material: L-Histidine Tetrafluoroborate," *J. Cryst. Growth*, Vol. 204, pp. 179–182, 1999.

48. Wang, W.S.; Aggarwal, M.D.; Choi, J.; et al.: "Solvent Effects and Polymorphic Transformation of Organic Nonlinear Optical Crystal L-Pyroglutamic Acid in Solution Growth Processes, I. Solvent Effects and Growth Morphology," *J. Cryst. Growth*, Vol. 198/199, pp. 578–582, 1999.

49. Owens, C.; Bhat, K.; Wang, W.S.; et al: "Bulk Growth of High-Quality Nonolinear Optical Crystals of L-Arginine Tetrafluoroborate (L–AFB)," *J. Cryst. Growth*, Vol. 225, pp. 465–469, 2001.

50. Lal, R.B.; Zhang, H.W.; Wang, W.S.; et al.: "Crystal Growth and Optical Properties of 4-Aminobenzophenone Crystals for NLO Applications," *J. Cryst. Growth*, Vol. 174, No. 1, pp. 393–397, 1997.

51. Zhang, H.W.; Batra, A.K.; and Lal, R.B.: "Growth of Large Methyl-(2,4-Dinitrophenyl)-Aminopropanoate: 2-Methyl-4-Nitroaniline Crystals for Nonlinear Applications," *J. Cryst. Growth*, Vol. 137, pp. 141–144, 1994.

52. Simmons, M.R.: "An Investigation of Crystals Matrices of Single Crystals Doped With Rare Earth Ions," Alabama A&M University, Normal, AL, 2002.

53. Chang, J.M.; Batra, A.K.; and Lal, R.B.: "Growth and Characterization of Doped TGS Crystals for Infrared Devices," *Cryst. Growth and Design*, Vol. 2, No. 5, pp. 431–435, 2002.

54. Lal, R.B.; and Aggarwal, M.D.: "Reciprocating Crystallizer: Automatic Crystallizer Grows Crystals From Aqueous Solutions," *NASA Tech. Briefs*, Vol. 8, p. 419, 1984.

55. Aggarwal M.D.; and Lal, R.B.: "Simple Low-Cost Reciprocating Crystallizer for Solution Crystal Growth," *Rev. Sci. Instr.*, Vol. 54, No. 6, pp. 772–773, 1983.

56. Batra, A.K.; and Mathur, S.C.: "Reciprocating Arrangement for Solution Crystal Growth," *Res. Indust.*, Vol. 20, p. 29, 1984.

57. Batra, A.K.; Carmichael-Owens, C.R.; Simmons, M.; et al.: "Design of a Solution Crystal Growth Crystallizer With Versatile Electronic Reciprocal Motion Control for a Crystal Holder," *Cryst. Res. Technol.*, Vol. 40, No. 8, pp. 757–760, 2005.

58. Batra, A.K.; Aggarwal, M.D.; and Lal, R.B.: "Growth and Characterization of Doped DTGS Crystals for Infrared Sensing Devices," *Mater. Lett.*, Vol. 57, No. 24–25, pp. 3943–3948, 2003.

59. Jona, F.; and Shirane, G.: *Ferroelectric Crystals*, Dover Publications Inc., New York, NY, 1993.

60. Lal, R.B.; and Batra, A.K.: "Growth and Properties of Triglycine Sulfate (TGS) Crystals: Review," *Ferroelectrics*, Vol. 142, pp. 51–82, 1993.

61. White, E.A.D.; Wood, J.D.C.; and Wood, V.M.: "The Growth of Large Area, Uniformly Doped TGS Crystals," *J. Cryst. Growth*, Vol. 32, pp. 149–156, 1976.

62. Brezina, B.; Havrankova, D.M.; and Vasa, M.: "Enhanced Growth of Nonpolar{001} Growth Sectors of Deuterated Triglycine Sulfate Doped With L-Alanine (LADTGS)," *Cryst. Res. Technol.*, Vol. 27, No. 1, pp. 13–20, 1992.

63. Satapathy, S.; Sharma, S.K.; Karnal, A.K.; and Wadhawan, V.K.: "Effect of Seed Orientation on the Growth of TGS Crystals With Large (010) Facets Needed for Detector Applications," *J. Cryst. Growth*, Vol. 240, No. 1–2, pp. 196–202, 2002.

64. Banan, M.: "Growth of Pure and Doped Triglycine Sulfate Crystals for Pyroelectric Infrared Detector Applications," Alabama A&M University, Normal, AL, 1986.

65. Zhao-De D.: "A New Method of Growth of Ferroelectric Crystal," *Ferroelectrics*, Vol. 39, p. 1237, 1981.

66. Moravec, F.; and Novotny, J.: "Study on the Growth of Triglycine Sulphate Single Crystals," *Kristall and Tecknik,* Vol. 7, pp. 891–902, 1972.

67. Burton, W.K.; Cabrera, N.; and Frank, F.C.: *Philos. Trans. R. Soc.*, London, Vol. 243, p. 299 1951.

68. Rashkovich, L.N.: *Sov. Phys. Crystallog.*, Vol. 28, p. 454, 1983.

69. Novotny, J.; Moravec, F.; and Solc, Z.: "The Role of Surface and Volume Diffusion in the Growth of TGS Single Crystals," *Czech. J. Phys.*, Vol. 23, No. 2, pp. 261–266, 1973.

70. Novotny, J.; and F. Moravec, F.: "Growth of TGS From Slightly Supersaturated Solutions," *J. Cryst. Growth,* Vol. 11, pp. 329–335, 1971.

71. Reiss, D.A.; Kroes, R.L.; and Anderson, E.E.: "Growth Kinetics of the (001) Face of TGS Below the Ferroelectric Transition Temperature," *J. Cryst. Growth*, Vol. 84, No. 1, pp. 7–10, 1987.

72. Moravec, F.; and Novotny, J.: "A Contribution to the Study of the Influence of Impurities on the Growth and Some Physical Properties of TGS Single Crystals," *Kristall and Technik*, Vol. 6, No. 3, pp. 335–342, 1971.

73. Whipps, R.V.; Cosier, R.S.; and Bye, K.L.: "Orthorhombic Diglycine Sulphate," *J. Mater. Sci.*, Vol. 7, No. 12, pp. 1476–1477, 1972.

74. Dominquez, E.; Jimenez, B.; Mendiola, J.; and Vivas, E.: "Diglycine Sulphate—An Interesting New Dielectric Crystal Species," *J. Mat. Sci.*, Vol. 7, No. 3, pp. 363–364, 1972.

75. Tsedrik, M.S.; Ulasen, V.N.; and Zaborovski, G.A.: "Growing of TGS and TGSe Single Crystals at Various pH of Solution," *Kristall and Technik*, Vol. 10, No.1, pp. 49–54, 1975.

76. Weidmann, E.J.; White, E.A.D.; and Wood, V.M.: "Induced Growth Anisotropy in TGS Crystals," *J. Mat. Sci. Lett.*, Vol 7, No. 6, pp. 719–720, 1972.

77. Szczepanska, L.: "Growth Investigations of Single Crystal Sulphates Containing Molecular Glycine Groups," *Kristall and Technik*, Vol. 11, No. 3, pp. 265–271, 1976.

78. Prokopova, L.; Novotny, J.; Micka, Z.; and Malina, V.: "Growth of Triglycine Sulphate Crystals Doped by Cobalt (II) Phosphate," *Cryst. Res. Technol.*, Vol. 36, No. 11, pp. 1189–1195, 2001.

79. Pandya, G.R.; and Vyas, D.D.: "On Growth and Morphological Studies of TGS Single Crystals," *Kristall and Technik*, Vol. 16, No. 12, pp. 1353–1358, 1981.

80. Lal, R.B.; Etminan, S.; and Batra, A.K.: "Effect of Simultaneous Organic and Inorganic Dopants on the Characteristics of Triglycine Sulfate Crystals," *Proc. 9th IEEE Intern. Symp. on Applications of Ferroelectrics*, University Park, PA, Vol. 7, pp. 695–697, 1994.

81. Banan, M.; Batra, A.K.; and Lal, R.B.: "Growth and Morphology of Triglycine Sulphate (TGS) Crystals," *J. Mat. Sci. Lett.*, Vol. 8, No. 11, pp. 1348–1349, 1989.

82. Banan, M.; Lal, R.B.; Batra, A.K.; and Aggarwal, M.D.: "Effect of Poling on the Morphology and Growth Rate of TGS Crystals," *Cryst. Res. Technol.*, Vol. 24, No. 3, pp. K53–K55, 1989.

83. Nakatani, N.: "Ferroelectric Domain Structure and Internal Bias Field in DL-α-Alanine-Doped Triglycine Sulfate," *Jpn. J. Appl. Phys.*, Vol. 30, No. 12R, pp. 3445–3449, 1991.

84. Eisner, J.: "The Physical Properties of TGS Single Crystals Grown From Aqueous TGS Solutions Containing Aniline," *Phys. Status Solidi*, Vol. 43, No. 1, pp. K1–K4, 1977.

85. Moravec, F.; Novotny, J.; and Strajblova, J.: "Single Crystals of Triglycine Sulphate Containing Palladium," *Czech. J. Phys.*, Vol. 23, No. 8, pp. 855–862, 1973.

86. Sidorkin, A.S.; and Kostsov, A.M.; and Tybulewicz, A.: "Exoelectron Emission From a Ferroelectric Crystal of Triglycine Sulfate With Defects," *Soviet Physics-Solid State,* Vol. 33, No. 8, pp. 1383–1384, 1991.

87. Yang, L.; Batra, A.K.; and Lal, R.B.: "Growth and Characterization of TGS Crystals Grown by Cooled Sting Technique," *Ferroelectrics*, Vol. 118, No. 1–4, pp. 85–91, 1991.

88. Nakatani, N.: "Ferroelectric Domain Structure and Internal Bias Field in DL-α-Alanine Doped Triglycine Sulfate," *Jap. J. Appl. Phys.*, Vol. 30, pp. 3445–3449, 1991.

89. Brezina, B.; and Havrankova, M.: "Orientation of Structure and Crystals of TGS and TGS Doped With D, Al, or L," *Cryst. Res. Technol.*, Vol. 20, No. 6, pp. 781–786, 1985.

90. Loiacono, G.M.; and Dougherty, J.P.: "Development and Verification of Pyroelectric Materials with Low Thermal Diffusivity," *Final Technical Report No. DAAK70–77–C–0098*, Philips Labs Inc., Briarcliff Manor, NY, 1978.

91. Wang, O.W.; and Fang, C.S.: "Investigation of the Solution Status of TGS and ATGSP Crystals," *Cryst. Res. Technol.*, Vol. 27, No. 2, pp. 245–251, 1992.

92. Seif, S.; Bhat, K.; Batra, A.K.; Aggarwal, M.D.; and Lal, R.B.: "Effect of Cr(III) Impurity on the Growth Kinetics of Potassium Dihydrogen Phosphate and Triglycine Sulfate Crystals Grown From Aqueous Solutions, *Mat. Lett.*, Vol. 58, No. 6, pp. 991–994, 2004.

93. Kuznetsov, V.A.; Okhrimenko, T.M.; and Rak, M.: "Growth Promoting Effect of Organic Impurities on Growth Kinetics of KAP and KDP Crystals," *J. Cryst. Growth*, Vol. 193, pp. 164–173, 1998.

94. Davey, R.J.: "The Control of Crystal Habit," *7th International Symposium on Industrial Crystallization*, Vol. 78, pp. 169–183, E. J. de Jong and S. J. Jancic (Eds), North-Holland, Amsterdam, 1979.

95. Meera, K.; Muralidharan, R.; Tripathi, A.K.; Ramasamy, P.: "Growth and Characterization of l-threonine, dl-threonine, and l-methionine Admixtured TGS Crystals," *J. Crystal Growth*, Vol. 263, pp. 524–531, 2004.

96. Su, G.; He, Y.; Yao, H.; et al.: "A New Pyroelectric Crystal L-Lysine-Doped TGS (LLTGS)," *J. Cryst. Growth*, Vol. 209, No. 1, pp. 220–222, 2000.

97. Arunmozhi, G.; De Matos, G.E.; and Ribeiro, J.: "Dielectric Properties of L-Asparagine Doped TGS (Asp-TGS) Crystals," *Ferroelectrics*, Vol. 295, No. 1, pp. 87–95, 2003.

98. Novotny, J.; Zelinka, J.; and Moravec, F.: "Broadband Infrared Detectors on the Basis of PATGS/Pt(IV) Single Crystals," *Sensors and Actuators*, Vol. 119, No. 2, pp. 300–304, 2005.

99. Kalainathan, S.; Margaret, M.B.; and Irusan, T.: "Morphological Changes of L-Asparagine Doped TGS Crystal," *Cryst. Engn.*, Vol. 5, No. 1, pp. 71–78, 2002.

100. http://www.nasa.gov/mission pages/shuttle/shuttlemissions/list main.html

101. Lal, R.B.; and Kroes, R.L.: "Solution Growth of Crystal on Spacelab-3," *Proceedings of the 24th AIAA Science Meeting*, Reno, NV, January 6–8, 1985.

102. Lal, R.B.; Aggarwal, M.D.; Kroes, R.L.; and Wilcox, W.R.: "A New Technique of Solution Crystal Growth," *Phys. Status Solidi*, Vol. 80, No. 2, pp. 547–552, 1983.

103. Batra, A.K.; Lal, R.B.; and Aggarwal, M.D.: "Electrical Properties of TGS Crystals Grown by New Technique," *J. Mat. Sci. Lett.*, Vol. 4, No. 11, pp. 1415–1418, 1985.

104. Lal, R.B.; Aggarwal, M.D.; Batra, A.K.; and Kroes, R.L.: "Solution Growth of Crystals in Zero-Gravity," Final Technical Report, *NASA Contract Number NAS8–32945*, 1987.

105. Yang, L.; Batra, A.K.; and Lal, R.B.: "Growth and Characteristics of TGS Crystals Grown by Cooled Sting Technique," *Ferroelectrics*, Vol. 118 No. (1–4), pp. 85–89, 1991.

106. Lal, R.B.; Batra, A.K.; Trolinger, J.D.; and Wilcox, W.R.: "TGS Crystal Growth Experiment on the First International Microgravity Laboratory (IML–1)," *Microgravity Quarterly*, Vol. 4, No. (3), pp. 186–198, 1994.

107. Lal, R.B.: "Solution Growth of Crystals in Low-Gravity," *NASA Contract Number NAS8–36634*, Final Technical Report, 1995.

108. Steiner, B.; Dobbyn, R.; Black, D.; et al.: "High-Resolution Diffracting Imaging of Crystals Grown in Microgravity and Closely Related Terrestrial Crystals," *NIST Technical Note 1287*, 1991.

109. McRee, D.E.: *Practical Protein Crystallography*, Academic Press, pp. 1–23, San Diego, CA, 1993.

110. Rhodes, G.: *Crystallography Made Crystal Clear,* Academic Press, pp. 8–10 and 29–38, San Diego, CA, 1993.

111. Durbin, S.D.; and Feher, G.: "Studies of Crystal Growth Mechanisms of Proteins by Electron Microscopy," *J. Mol. Biol.*, Vol. 212, pp. 763–774, 1990.

112. Forsythe, E.; and Pusey, M.L.: "The Effects of Temperature and NaCl Concentration on Tetragonal Lysozyme Face Growth Rates," *J. Cryst. Growth*, Vol. 139, pp. 89–94, 1994.

113. Nadaraja, A.; Forsythe, E.L.; and Pusey, M.L.: "The Averaged Face Growth Rates of Lysozyme Crystals: The Effect of Temperature," *J. Cryst. Growth*, Vol. 151, pp. 163–172, 1995.

114. Littke, W.; and John, C.: "Protein Single Crystal Growth Under Microgravity," *Science*, Vol. 225, pp. 203–204, 1984.

115. Rosenberger, F.: "Protein Crystallization," *J. Cryst. Growth*, Vol. 166, pp. 40–54, 1996.

116. Gorti, S.; Forsythe, E.L.; and Pusey, M.L.: "Measurable Characteristics of Lysozyme Crystal Growth," *Acta Cryst.*, Vol. D61, pp. 837–843, 2005.

117. http://science.nasa.gov/ssl/msad/pcg/

118. Littke, W.; and John, C.: "Protein Single Crystal Growth Under Microgravity," *J. Cryst. Growth*, Vol. 76, pp. 663–672, 1986.

119. DeLucas, L.J.; Suddath, F.L.; Snyder, R.S.; et al.: "Preliminary Investigations of Protein Crystal Growth Using the Space Shuttle," *J. Cryst. Growth*, Vol. 76, pp. 681–693, 1986.

120. DeLucas, L.J.; Smith, C.D.; and Smith, H.W.; et al.: "Protein Crystal Growth in Microgravity," *Science*, Vol. 246, pp. 651–653, 1989.

121. Simic-Stefani, S.; Kawaji, M.; and Hu, H.U.: "G-Jitter Induced Motion of a Protein Crystal Under Microgravity," *J. Cryst. Growth*, Vol. 294, pp. 373–384, 2006.

122. McPherson, A.: "Virus and Protein Crystal Growth on Earth and in Microgravity," *J. Phys.*, Vol. D, No. 26, pp. B104–B112, 1993.

123. Carter, D.C.; and Dowling, T.E.: "Protein Crystal Growth Apparatus for Microgravity," U.S. Patent No. 5,643,540, 1997.

124. Carter, D.C.; Wright, B.; Miller, T.; et al.: "PCAM: A Multiuser Facility-Based Protein Crystallization Apparatus for Microgravity," *J. Cryst. Growth*, Vol. 196, pp. 610–622, 1999.

125. Carter, D.C.; Wright, B.; Miller, T.; et al.: "Diffusion-Controlled Crystallization Apparatus for Microgravity (DCAM): Flight and Ground-Based Applications," *J. Cryst. Growth*, Vol. 196, pp. 602–609, 1999.

126. DeLucas, L.J.; Moore, K.M.; Long, M.M.; et al.: "Protein Crystal Growth in Space, Past and Future," *J. Cryst. Growth*, pp. 237–239 and 1646–1650, 2002.

127. Declereq, J.P.; Evrard, C.; Carter, D.C.; et al.: "A Crystal of a Typical EF-Hand Protein Grown Under Microgravity Diffracts X-Rays Beyond 0.9 A Resolution," *J. Cryst. Growth*, Vol. 196, pp. 595–601, 1999.

128. Carter, D.C.; Lim, K.; Ho, J.X.; Wright, B.S.; et al.: "Lower Dimmer Impurity Incorporation May Result in Higher Perfection of HEWL Crystals Grown in Microgravity: A Case Study," *J. Cryst. Growth*, Vol. 196, pp. 623–637, 1999.

REPORT DOCUMENTATION PAGE

Form Approved
OMB No. 0704-0188

1. AGENCY USE ONLY *(Leave Blank)*	2. REPORT DATE	3. REPORT TYPE AND DATES COVERED
	December 2007	Technical Memorandum

4. TITLE AND SUBTITLE

Solution Growth and Characterization of Single Crystals on Earth and in Microgravity

5. FUNDING NUMBERS

NNG06GC58A

6. AUTHORS

M.D. Aggarwal, J.R. Currie, B.G. Penn, A.K. Batra*, and R.B. Lal*

7. PERFORMING ORGANIZATION NAME(S) AND ADDRESS(ES)

George C. Marshall Space Flight Center
Marshall Space Flight Center, AL 35812

8. PERFORMING ORGANIZATION REPORT NUMBER

M–1211

9. SPONSORING/MONITORING AGENCY NAME(S) AND ADDRESS(ES)

National Aeronautics and Space Administration
Washington, DC 20546–0001

10. SPONSORING/MONITORING AGENCY REPORT NUMBER

NASA/TM—2007–215187

11. SUPPLEMENTARY NOTES

*Alabama A&M University, Department of Physics, P.O. Box 1268 Normal, AL 35762
Prepared by the Spacecraft and Vehicle Systems Department Engineering Directorate

12a. DISTRIBUTION/AVAILABILITY STATEMENT

Unclassified-Unlimited
Subject Category 29
Availability: NASA CASI 301–621–0390

12b. DISTRIBUTION CODE

13. ABSTRACT *(Maximum 200 words)*

Crystal growth has been of interest to physicists and engineers for a long time because of their unique properties. Single crystals are utilized in such diverse applications as pharmaceuticals, computers, infrared detectors, frequency measurements, piezoelectric devices, a variety of high-technology devices, and sensors. Solution crystal growth is one of the important techniques to grow a variety of crystals when the material decomposes at the melting point and a suitable solvent is available to make a saturated solution at a desired temperature. In this Technical Memorandum (TM) an attempt is made to give the fundamentals of growing crystals from solution including improved designs of various crystallizers. Since the same solution crystal growth technique could not be used in microgravity, the authors proposed a new cooled-sting technique to grow crystals in space. The authors' experience from conducting two Space Shuttle solution crystal growth experiments are also detailed in this TM and the complexity of solution growth experiments to grow crystals in space are also discussed. These happen to be some of the early experiments performed in space, and various lessons learned are described. A brief discussion of protein crystal growth that shares basic principles of the solution growth technique is given, along with some flight hardware information for growth in microgravity.

14. SUBJECT TERMS

Solution crystal growth, microgravity, triglycine sulfate, protein crystals, Spacelab-3, International Microgravity Laboratory-1

15. NUMBER OF PAGES

64

16. PRICE CODE

17. SECURITY CLASSIFICATION OF REPORT	18. SECURITY CLASSIFICATION OF THIS PAGE	19. SECURITY CLASSIFICATION OF ABSTRACT	20. LIMITATION OF ABSTRACT
Unclassified	Unclassified	Unclassified	Unlimited

National Aeronautics and
Space Administration
IS20
George C. Marshall Space Flight Center
Marshall Space Flight Center, Alabama
35812